

UNCLASSIFIED

AD NUMBER
AD478552
NEW LIMITATION CHANGE
TO Approved for public release, distribution unlimited
FROM Distribution authorized to U.S. Gov't. agencies only; Administrative/Operational Use; FEB 1966. Other requests shall be referred to Office of Naval Research, 875 North Randolph Street, Arlington, VA 22203.
AUTHORITY
ONR ltr dtd 28 Jul 1977

THIS PAGE IS UNCLASSIFIED

THIS REPORT HAS BEEN DELIMITED
AND CLEARED FOR PUBLIC RELEASE
UNDER DOD DIRECTIVE 5200.20 AND
NO RESTRICTIONS ARE IMPOSED UPON
ITS USE AND DISCLOSURE.

DISTRIBUTION STATEMENT A

APPROVED FOR PUBLIC RELEASE;
DISTRIBUTION UNLIMITED.

Final Report

THE GENERATION OF MEGAWATT PEAK POWERS
BY MODERN SPARK-TRANSMITTER TECHNIQUES

By: L. T. DOLPHIN, JR. A. F. WICKERSHAM, JR.

Prepared for:

OFFICE OF NAVAL RESEARCH
WASHINGTON, D.C.
AND
ADVANCED RESEARCH PROJECTS AGENCY
WASHINGTON, D.C.

CONTRACT Nonr-4178(00)
ARPA ORDER NO. 463

STANFORD RESEARCH INSTITUTE

MENLO PARK, CALIFORNIA

*SRI

478552

OPY

ACCESSION No.		
CPSTI	WHITE SECTION	<input type="checkbox"/>
DDO	DIFF SECTION	<input checked="" type="checkbox"/>
UNCLASSIFIED	STATEMENT	<input checked="" type="checkbox"/>
JUSTIFICATION	<i>on Doc</i>	
BY <i>fm</i>		
DISTRIBUION/AVAILABILITY CODES		
UNCL.	REST.	CONF. SPECIAL
<i>3</i>		

"Research Supported by the Advanced Research Projects Agency, ARPA Order 463, through the Office of Naval Research, Contract NONr-4178(00), Task No. NR 088-023."

"U.S. Government Agencies may obtain copies of this report from DDC. Other qualified DDC users shall request through the Office of Naval Research, Field Projects Branch."



Form 1473

(11) Feb 1966,
(12) 70p.

(9) Final Report

(6) THE GENERATION OF MEGAWATT PEAK POWERS
BY MODERN SPARK-TRANSMITTER TECHNIQUES

Prepared for:

OFFICE OF NAVAL RESEARCH
WASHINGTON, D.C.
AND
ADVANCED RESEARCH PROJECTS AGENCY
WASHINGTON, D.C.

(15)
Nonr-4178(00)
ARPA ORDER 463

(10) Lambert T. DOLPHIN, JR. and thur
AFF. WICKERSHAM, JR.

(16) SRI-4548

(17) NR-088-023

This Project was sponsored by the Advanced Research Projects Agency as part of Project DEFENDER under ARPA Order No. 463.

The reproduction of this report in whole or in part is permitted for any purpose of the United States Government.

Approved: R. L. LEADABRAND, MANAGER
RADIO PHYSICS LABORATORY

D. R. SCHEUCH, EXECUTIVE DIRECTOR
ELECTRONICS AND RADIO SCIENCES

Copy No. 88

18

ABSTRACT

The demand for greater peak power for pulse radars has prompted the application of modern technology to the spark-gap transmitters of many years ago; in addition, working models have been built and tested of a spark transmitter recently invented in Australia.

Working models have been tested at 6, 12, 23, 90, and 100 MHz with peak powers of 1/2 to 5 MW. The initial phase of a spark transmitter has been controlled to within 0.2 nsec, permitting pulse-to-pulse coherence for Doppler radar. A pulse radar has been built using a 6 MHz spark transmitter; the output power, spectrum, and efficiency have been determined, and multiple ionospheric echoes have been observed. Bandwidth is about what would be expected for a pulse typically 1 μ s long at 20 MHz. The spectrum is reasonably free of noise and harmonics; efficiencies lie between 10 and 25 percent.

We conclude that peak powers as large as several gigawatts are possible. High-power operation may be achieved at frequencies as high as 100 to 200 MHz, and initial phase can be controlled to within a few tenths of a nanosecond.

A 1 to 5 MW radar system using spark transmitters at 6, 12, and 23 MHz is now under construction.

CONTENTS

ABSTRACT	iii
LIST OF ILLUSTRATIONS	vii
LIST OF TABLES	ix
I. INTRODUCTION	1
II. THE SPARK-RING TRANSMITTER	5
III. CYLINDRICAL TRANSMITTERS	19
IV. INSTRUMENTATION AND TESTING	27
V. CONCLUSION	45
ACKNOWLEDGEMENTS	55
REFERENCES	57

ILLUSTRATIONS

Fig. 1	Spark Oscillator Configurations	2
Fig. 2	20 MHz Ring Transmitter Section	7
Fig. 3	20 MHz Ring Transmitter	8
Fig. 4	Small UHF Ring Transmitter	10
Fig. 5	Yagi Array Excited by a Small UHF Spark Ring	11
Fig. 6	Empirically Determined Design of a Yagi Array Excited by a Small Spark Ring	12
Fig. 7	Section of a Ring Transmitter with Pressurized Spark-Gap Units	14
Fig. 8	Oscillogram Showing the Voltage Waveform Transmitted by the 23 MHz Spark Ring	15
Fig. 9	Photograph of Two Configurations of Triggered Pressurized Spark Gaps	16
Fig. 10	150 MHz Ring Transmitter	20
Fig. 11	Simplified Sketch of Franklin's Invention for Generating HF Radio Energy	21
Fig. 12	Schematic Drawing of a Means of Generating High-Power UHF Radio Pulses	22
Fig. 13	20 MHz Cylindrical Generator	23
Fig. 14	90 MHz Cylindrical Generator with Dipole Radiator	24
Fig. 15	Photograph of a 100 MHz Cylindrical Generator with an Asymmetrical Slot Radiator Cut Parallel to the Axis	25
Fig. 16	Early Model of the Ring Transmitter and a Shorted, Parasitic, Secondary Ring	28
Fig. 17	Pulse Waveform from the Pressurized 23 MHz Ring Transmitter	29
Fig. 18	A-Scope Presentation of Clutter Echoes from the 23 MHz Transmitter	29
Fig. 19	A Portion of the Fast-Pulse Ultraviolet Triggering Circuit	29

ILLUSTRATIONS (Concluded)

Fig. 20	Oscillogram of Superimposed Pulses from the Triggering Spark Gaps	30
Fig. 21	Schematic Diagram of the Delayed-Pulse Triggering Circuit Used with the 6 MHz Ring Transmitters	32
Fig. 22	6 MHz Spark-Ring Transmitter	33
Fig. 23	Two Driver (Active) 6 MHz Ring Transmitters Coupled to a Shorted, Parasitic 6 MHz Ring and a Fourth, Larger Tuned Ring	34
Fig. 24	RF Pulses from a 6 MHz Ring Transmitter	35
Fig. 25	RF Pulses from a 6 MHz Ring Transmitter, Showing the Effect of Coupling a High-Q, Tuned, Secondary Ring to the Driver Ring	36
Fig. 26	6 MHz Radiated Signal, Showing Pulse-to-Pulse Jitter ($PRF \approx 1$ pps)	37
Fig. 27	Combined RF Pulses from Two Active, 6 MHz Rings (No Parasitic Ring)	38
Fig. 28	Combined RF Pulses from Two Active, 6 MHz Rings, Using a Third, Parasitic Ring	39
Fig. 29	Junction of Pulses from Two 6 MHz Ring Transmitters	40
Fig. 30	F-Layer Echoes Obtained with the 6.6 MHz Ring-Transmitter System	41
Fig. 31	12 MHz Ring Transmitter Shown Mounted on Radome Platform	43
Fig. 32	Ring-Transmitter Radar System at 6, 12, and 24 MHz	44
Fig. 33	Artist's Conception of a Portable UHF Field Radar	47
Fig. 34	Proposed Form of a 50 MW, VLF Pulse Transmitter	49
Fig. 35	Radiation Resistance of a Rectangular Half-Loop over a Ground Plane	50
Fig. 36	H-Plane Radiation Patterns, Vertical Polarization, for a Rectangular Loop over a Ground Plane, for Various Distances of Separation of the Vertical Sides, Measured in Wavelengths	51
Fig. 37	E-Plane Radiation Pattern, Vertical Polarization, for a Vertical Loop over a Ground Plane for Various Distances of Separation of the Vertical Sides, Measured in Wavelengths	52
Fig. 38	Sketch of the Possible Appearance of a Megawatt CW, HF Transmitter	53

TABLES

Table I	Design Characteristics of 20 MHz Spark-Ring Transmitter	6
Table II	Ring-Transmitter Radar System Parameters	42

I INTRODUCTION

The electrical oscillations associated with the discharge of a capacitor were known to Joseph Henry as early as 1840, but the nature of the oscillations was not understood until Hertz, in 1888, used spark gap oscillators to demonstrate the wave character of electromagnetic radiation.

The hertzian oscillator may be regarded as the earliest spark gap transmitter. It consisted of a capacitor formed by two collinear conductors which were separated slightly at the center to form a spark gap, as shown in Fig. 1(a). The conductors were charged until the gap broke down and caused an oscillatory discharge of the capacitor through the spark channel. Since the capacitor was in the form of an electric dipole, the hertzian oscillator was an efficient radiator; however, its small capacitance precluded high-power operation. With reduced gap separation it also served as a receiver or detector.

The hertzian oscillator was the forerunner of a host of various types of spark transmitters that were developed after the turn of the century. We shall report here the progress made in the last three years toward building high-frequency spark transmitters having performance and power capability possibly greater than that achievable by other means at this time.

Although Hertz succeeded in generating microwave frequencies, early practical spark transmitters radiated significant power only at frequencies of tens or hundreds of kilohertzes. Thirty years ago frequencies as high as half a megahertz were achieved with the Poulsen arc generator. At the present time spark transmitters can be used to generate megawatt peak powers at frequencies of hundreds of megahertzes.

When vacuum tubes were invented, the spark transmitter was abandoned to steamship emergency rooms and laboratory cellars, and many of the novel schemes suggested during spark days were never carried further.

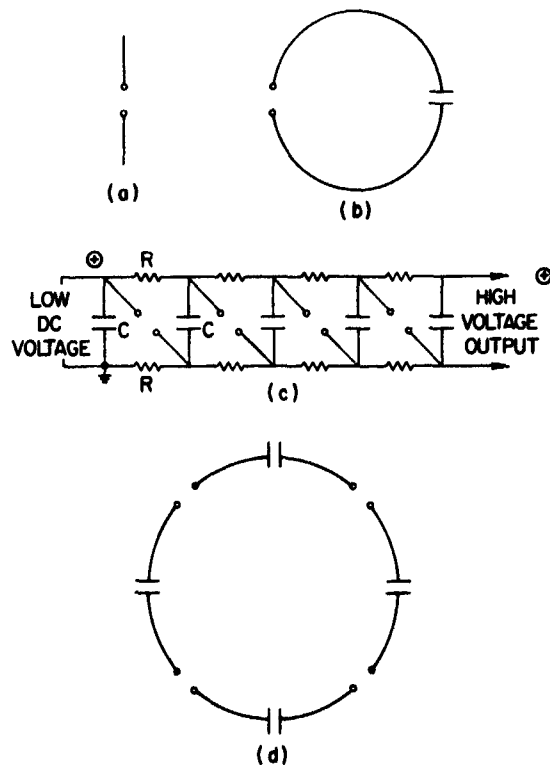


FIG. 1 SPARK OSCILLATOR CONFIGURATIONS
 (a) Hertzian Oscillator
 (b) Loop Oscillator
 (c) Marx Generator
 (d) Landecker Spark-Ring Transmitter

At the present time vacuum tubes are being pushed to higher power levels only at great expense and effort. Vacuum tubes are inherently inefficient, high-impedance devices, and peak power levels of most transmitting tubes are limited to a few megawatts. The demand for higher peak powers, particularly for radars, has prompted our investigation of other techniques for generating radio power.

A tubless device for generating very large peak powers was proposed in 1960 by Landecker and Imrie in Australia.^{1*} It is a type of spark transmitter similar to a Marx generator [Fig. 1(c)] in that capacitors are charged in parallel and discharged in series. In the next

* References are given at the end of this report.

section we shall describe Landecker's spark-ring transmitter and the performance of models built at this laboratory. There is no difficulty in constructing ring transmitters capable of radiating spectrally clean pulses at frequencies of tens of megahertz and with peak powers of 5 to 10 MW or more. Higher powers can be achieved at lower frequencies. In a later section we shall describe another spark-gap device capable of megawatt peak powers at frequencies of hundreds of megahertz.

II THE SPARK-RING TRANSMITTER

The hertzian oscillator is limited in power by the small capacitance of its collinear conductors. Energy storage can be increased by replacing the electric dipole with a magnetic dipole or loop configuration and using the loop to discharge a capacitor [Fig. 1(b)]. Radiation from the loop oscillator can be described by relatively simple equations: its angular frequency is $\omega = (LC)^{-1/2}$, where C is the capacitance and L the inductance of the loop, and the pulse length is governed by an exponential damping factor, the reciprocal of the coefficient in the exponent being the quality, $Q = \omega L/R$. The resistance, R, is the sum of the radiation resistance and the ohmic equivalent of the Joule heating losses in the conductor, in the spark channel, and in dielectric hysteresis. The energy available in a loop oscillator, $1/2CV^2$, can be quite large for large capacitors; however, if high frequencies are desired, the loop inductance must be kept small. The small inductance requirement so severely limits the physical size of the capacitor that ultimate frequency-power performance is disappointing.

The small inductance requirement at high frequencies is satisfied to a large extent by the Landecker ring transmitter. In the Landecker invention many capacitors are arranged in a circle, charged in parallel, and discharged in series through spark gaps [Fig. 1(d)]. In this scheme large series potentials of many megavolts can be achieved even though the charging potentials are only tens of kilovolts. By packing the capacitors closely, the lead length of each capacitor can be made very short since it does not, by itself, complete a circuit; thus, the lead inductance can be small and the operating frequency high at high peak powers. The equations for a ring transmitter with n capacitors are the same as those for a loop oscillator except that the capacitance is now the total series capacitance around the ring, C/n, and the energy storage is $1/2nCV^2$. The

basic design principle of the spark-ring transmitter requires the inductance of a single loop antenna to be tuned to resonance by the total series capacitance distributed around the loop.

One of the first ring transmitters built at this laboratory was designed to operate at 20 MHz . The design characteristics are given in Table I. Also shown are the characteristics of a secondary, passive ring, which eventually was used to increase the Q and pulse length of the overall transmitter. This transmitter was first tested in a simple configuration and then modified extensively in attempts to make it work.

Table I
DESIGN CHARACTERISTICS OF 20 MHz SPARK-RING TRANSMITTER

Parameter	Primary Ring	Secondary Ring
Number of capacitors	67	40
Capacitance per unit	356 ± 1 pF	356 ± 1 pF
Inductance of total ring	11 μ H	7.1 μ H
Capacitance of all units in series	5.3 pF	8.9 pF
Charging voltage	20-120 kV	0
Energy storage at 50 kV	30 Joules	0
Theoretical peak power averaged over transmitted pulse at 50 kV	17 MW	--
Pulse length	1.0 μ s	
Quality, Q	65	150
Ring diameter	2.9 m	2.0 m
Theoretical radiation resistance	23.3 Ω	4.66 Ω

The construction details are shown in Fig. 2. The capacitors were made of 1/8-inch copper-clad fiberglass laminate, which is commercially available and has a loss factor less than 0.009, a dielectric constant of 4.8, and a dielectric strength of 65 kV per 1/16 inch. The capacitors were charged through resistors made of plastic tubing filled with tap water. Resistances of 1 to 20 M Ω were obtained by changing the tubing size or adding a little salt to the water. The plastic tubing can be seen as spokes in Fig. 3, a photograph of the completed ring.

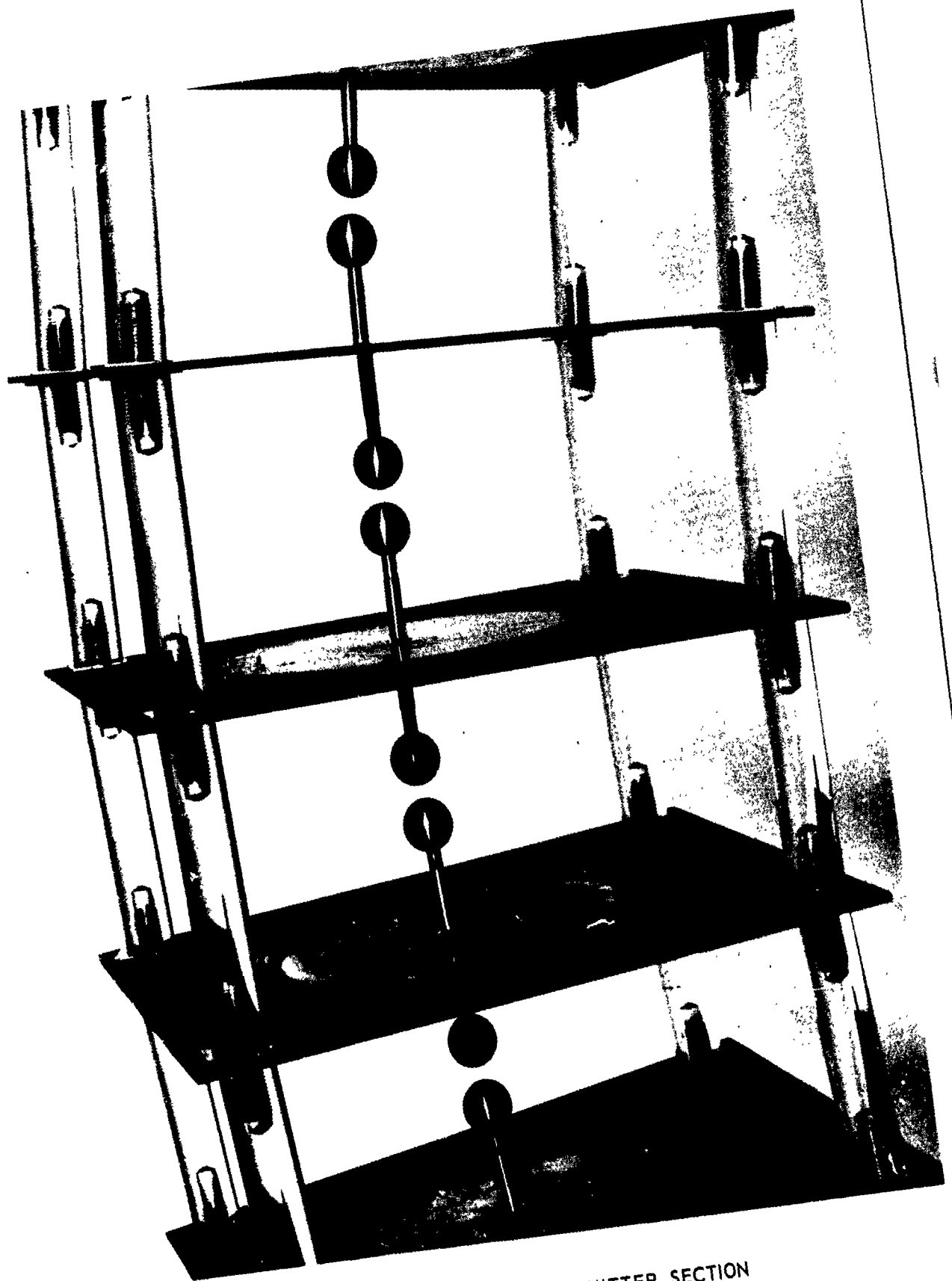


FIG. 2 20 MHz RING TRANSMITTER SECTION

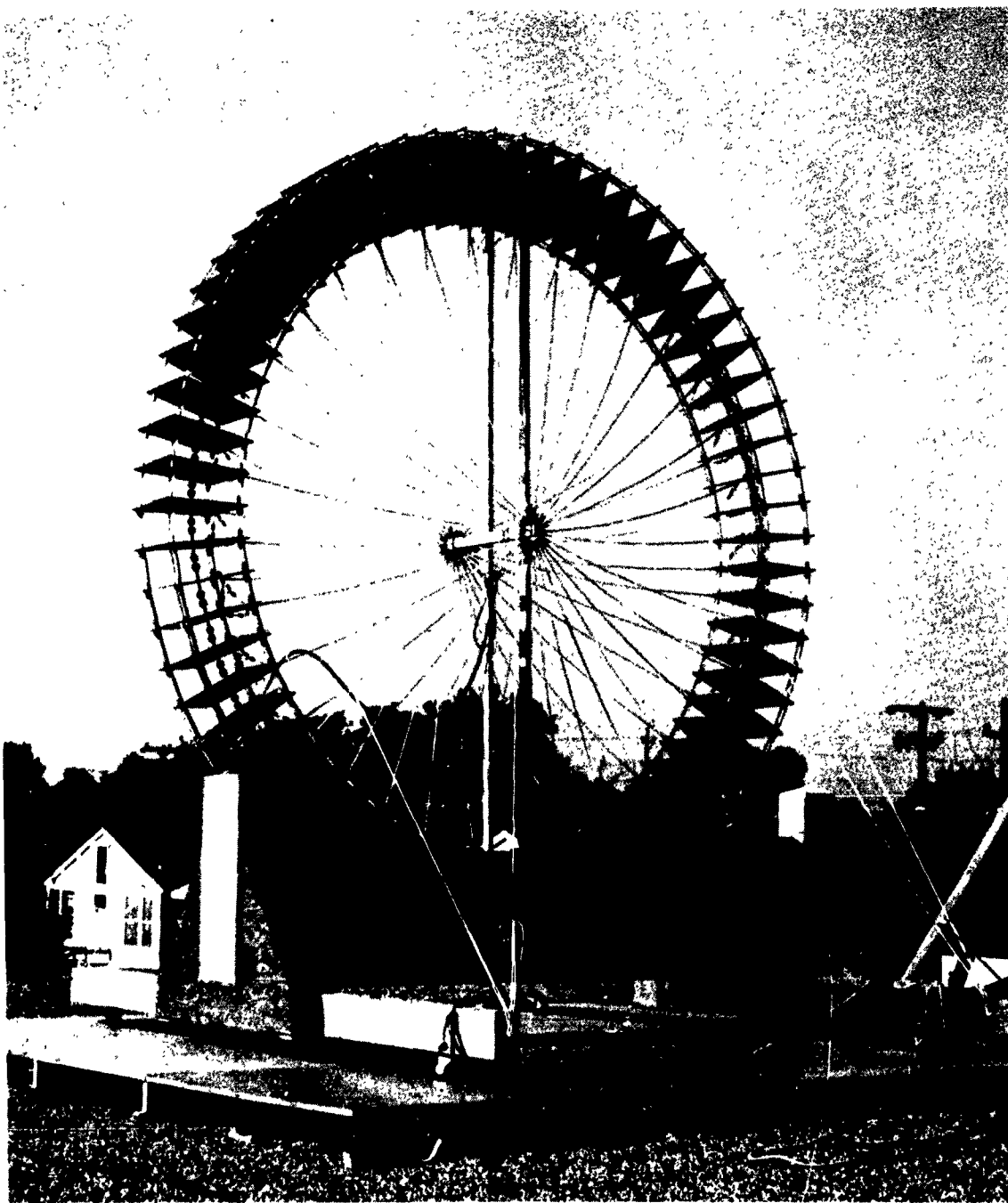


FIG. 3 20 MHz RING TRANSMITTER

The ring was ready for testing early in 1964, and for this purpose we set up a receiving station at the Stanford University field site, 5.6 km from the transmitter. We found the pulse width to be about 1 μ s, as expected, and obtained weak echoes from nearby mountains and aircraft. The measured power at 23 MHz, as obtained from the field strength of the direct signal at the receiver site, was only a few kilowatts--about three orders of magnitude less than expected. The frequency spectrum of the signal was diffuse, noiselike, and extensive, consisting mainly of two broad, overlapping maxima, near 23 and 32 MHz, and numerous harmonics.

At this time we also built and tested a small 370 Mc/s ring transmitter to determine performance at ultra-high frequencies and to gain experience in coupling a ring transmitter to parasitic elements. Figure 4 is a photograph of the UHF ring, and the use of the ring as the exciting element in a Yagi array is shown in Fig. 5. We had no difficulty in achieving satisfactory array performance for short arrays. An empirically determined design is shown in Fig. 6. However, for longer arrays the directivity was below that expected because of the broad frequency spectrum and short coherence length of the radiation. In making pattern measurements of the ring itself we found that axial radiation was only slightly less than radiation in the plane of the ring. Since an omnidirectional coherent source is impossible, we hypothesized that the radiation was largely incoherent and that the incoherency, in turn, derived from a randomness in spark-channel formation with respect to time intervals comparable to the period of oscillation.

The incoherency hypothesis was also consistent with the observed behavior of the 20 MHz transmitter. We found, after further study, that the resonant frequency of a single module--a single capacitor and its associated conductor and spark gap--was about 32 MHz. If the spark channels are formed randomly in time, individual modules or groups of modules can oscillate independently at the self-resonant frequency of 32 MHz; only when all channels are formed simultaneously is there an effective loop mutual inductance that lowers the resonant frequency to 23 MHz. We used two methods to determine the spark channel dynamic

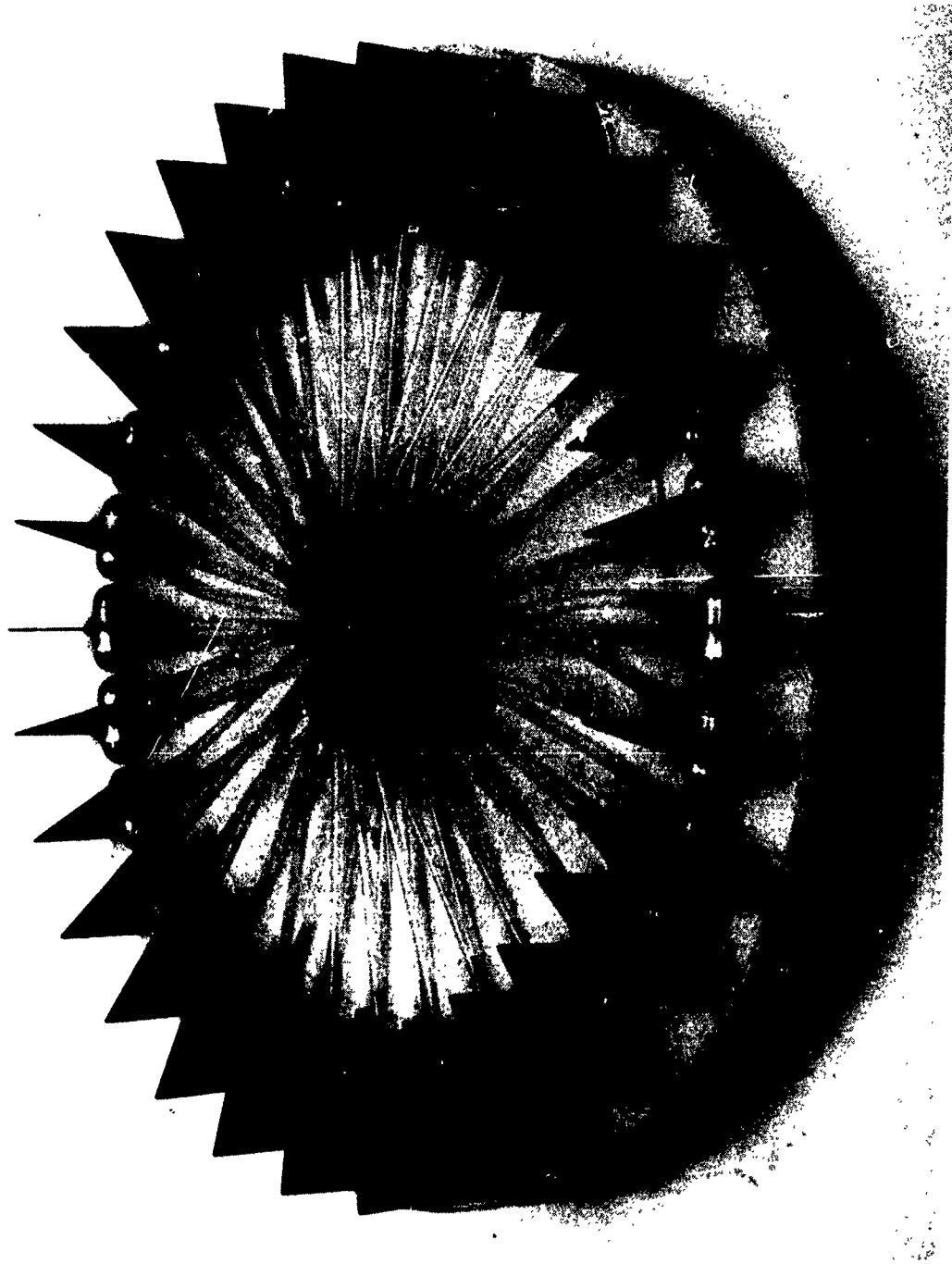


FIG. 4 SMALL UHF RING TRANSMITTER

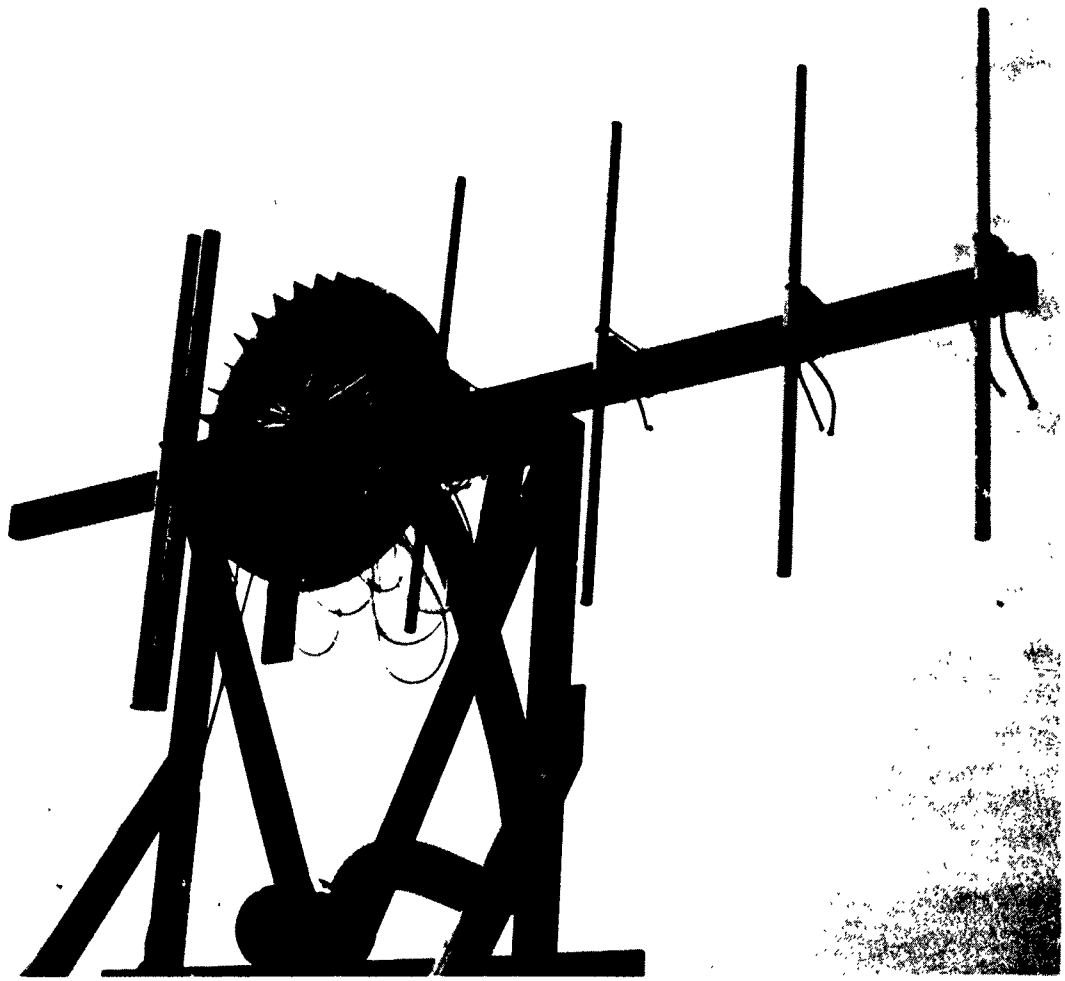


FIG. 5 YAGI ARRAY EXCITED BY A SMALL UHF SPARK RING

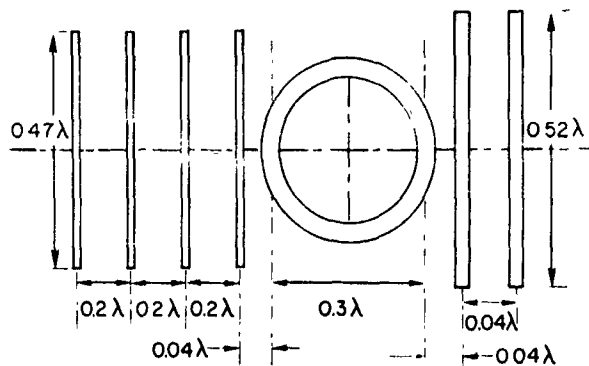


FIG. 6 EMPIRICALLY DETERMINED DESIGN
OF A YAGI ARRAY EXCITED
BY A SMALL SPARK RING

resistance and found that it was from 1 to 4 ohms per gap. We concluded that about one order of magnitude of power was lost in heating the spark channels and the remaining loss of about two orders of magnitude of power resulted from a lack of synchronization of the spark gaps.

Lack of synchronization was verified by using a streak camera to measure the jitter time between neighboring spark gaps. We found an average jitter time (time between formation of channels in neighboring gaps) of 115 ± 2 ns. Since coherent radiation at 20 MHz requires gap synchronization to within at least 5 ns, it is evident that air-gap ring transmitters are impractical at high frequencies.

Fortunately, the well-known pressurization technique for reducing spark-gap resistance also reduces channel formation time and thus synchronizes the spark gaps to a large extent. The use of pressurized gaps at 5 or 6 atmospheres permits a smaller gap spacing--typically about 0.05 cm--for a given charging voltage. The resultant spark is thicker and shorter. Since the energy is concentrated in a smaller volume of gas, the ion concentration is increased and the spark-channel resistance is reduced; also, shorter gap spacing speeds spark-channel formation and reduces the jitter-time problem. Accordingly, we installed 67 pressurized gaps in the 20 MHz rings. Each gap was enclosed in a plastic cylinder that could be pressurized with up to 6 atmospheres of nitrogen. A photograph of a section of

the pressurized ring is shown in Fig. 7. With the pressurized gaps we found more than an order of magnitude increase in radiated RF power and a corresponding sharpening of the frequency spectrum near 23 MHz. We subsequently achieved an additional order of magnitude by also providing each gap with a pair of auxiliary triggering electrodes.

All the auxiliary electrodes are connected in parallel so that they can be simultaneously activated by a fast-rise-time pulse. When a fast pulse is discharged through the auxiliary electrodes it produces an ultraviolet flash near each main spark gap. The ultraviolet light is absorbed in the gas near the electrodes and at the surface of the electrodes, and the absorption process generates free electrons. The availability of free electrons immediately starts the breakdown process; in addition, the volume ionization of the gas is equivalent to an overvolting of the main electrodes. The overvolting provides for a fast streamer type of breakdown, rather than the slower regenerative type. In order to enhance the number of free electrons generated by the ultraviolet flash, we used aluminum electrodes in the main spark gaps. Aluminum has the lowest surface work function of the readily available metals; in other words, it requires less energy to remove an electron from the surface of aluminum than from most other metals.

The increase in RF power with a trigger system is shown clearly in Fig. 8. This figure is an oscillogram showing voltage sweeps obtained from the 23 MHz ring transmitter. The receiving antenna was a monopole located on the roof of a building 326 feet away from the ring. The transmission line from the monopole was connected to a matched load directly across the deflection plates of the oscilloscope. The sweep speed of the oscilloscope was 100 ns/division, and one division on the vertical axis corresponds to 66 volts across the 50 Ω load. The first three sweeps were taken during normal, triggered transmission. The triggering system was then turned off and the ring allowed to discharge spontaneously for the last two sweeps shown in the photograph. The drop in amplitude corresponds to a power decrease of 12 dB, where all operating conditions are identical except for the stopping of the trigger system.

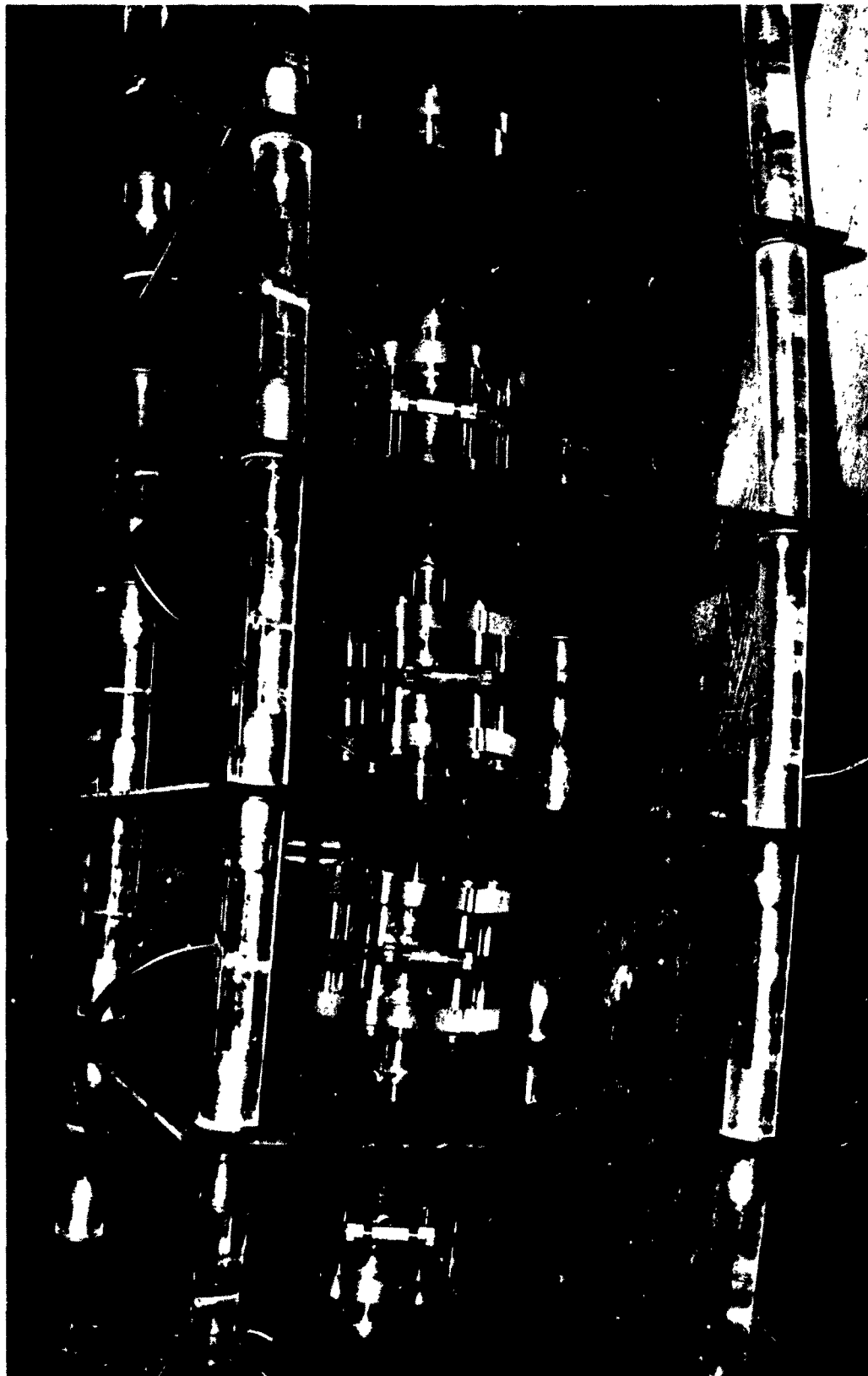


FIG. 7 SECTION OF A RING TRANSMITTER WITH PRESSURIZED SPARK-GAP UNITS

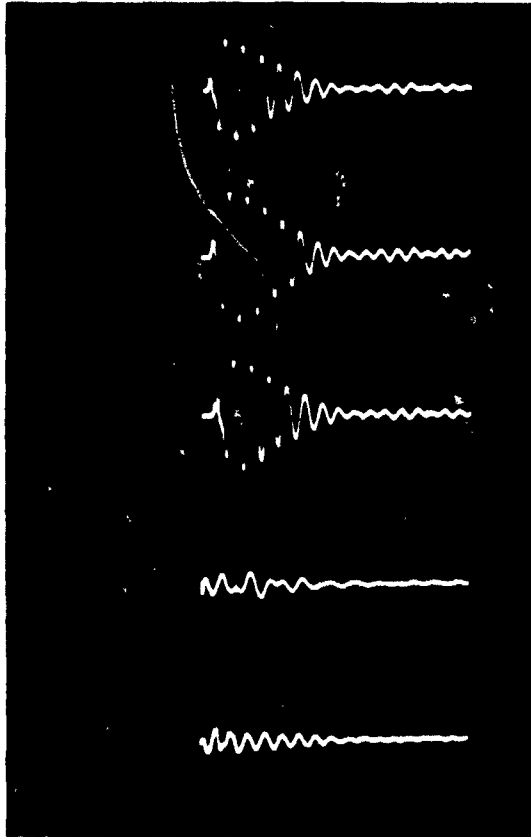


FIG. 8 OSCILLOGRAM SHOWING THE
VOLTAGE WAVEFORM TRANSMITTED
BY THE 23 MHz SPARK RING
Horizontal scale, 100 ns/division;
vertical scale, 66 volts/division.

Two examples of triggered spark gaps are shown in Fig. 9. The pressurized containers are constructed of transparent insulating material for convenience in inspection. In the rectangular configuration the main electrodes can be seen through the machined plastic. At right angles to the main electrodes there are two interconnecting cylindrical cavities. One leads to a pressure fitting and the other contains the two auxiliary or trigger electrodes. Only the upper trigger electrode can be seen clearly in the photograph. In the cylindrical configuration, in the lower

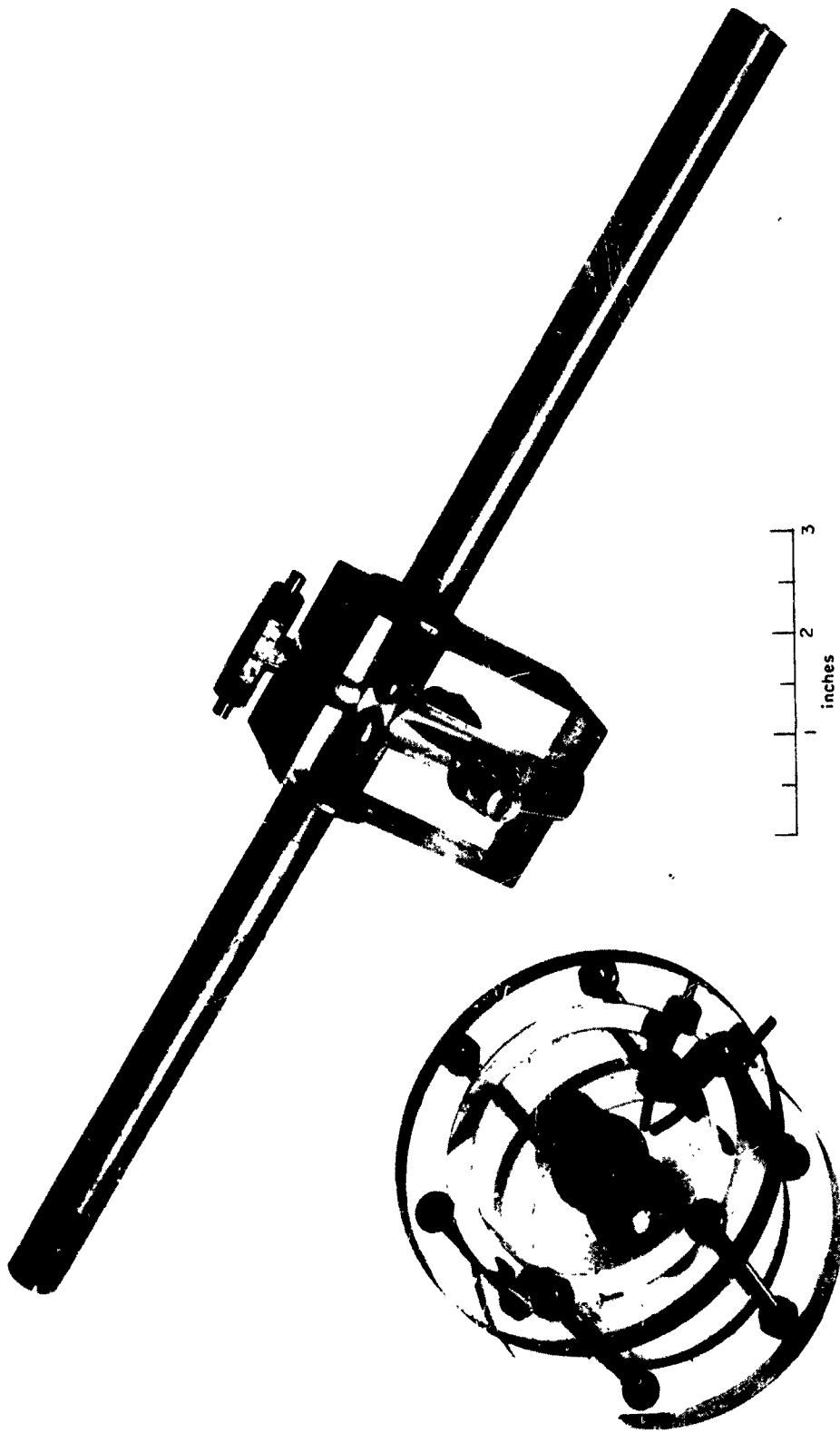


FIG. 9 PHOTOGRAPH OF TWO CONFIGURATIONS OF TRIGGERED PRESSURIZED SPARK GAPS

left corner of the photograph, the polished aluminum surface of the lower main electrode can be seen clearly just below the back side of the upper main electrode. The trigger electrodes can be seen on the right-hand side of the cylinder. These gaps have been operated successfully at about 40 psi (about 3 atmospheres) of nitrogen, and have been used in 6 and 23 MHz ring transmitters. In the 100 MHz cylindrical transmitters, which will be discussed next, we have used gaps pressurized to 180 psi (about 13 atmospheres). The triggered gaps not only permit synchronization of the elements of a transmitter, but also permit pulse-to-pulse coherency of the RF energy, an important requirement for radar Doppler measurements. The fast-rise-time pulse that simultaneously activates all of the trigger spark gaps can be generated by discharging a capacitor through a sharpening gap in a coaxial line, the discharge being initiated by a grid-controlled thyratron.

III CYLINDRICAL TRANSMITTERS

The basic principle of the Landecker ring (loop inductance tuned to resonance by capacitance distributed around the ring) cannot be extended to UHF without serious reduction of power capability. For example, a 150 MHz ring (Fig. 10) was built and tested that had a storage capacity of about 0.05 J. At 10 percent efficiency it radiated a peak power of only 50 kW.

In order to store more energy and at the same time keep inductance small, it is advantageous to use a cylindrical or coaxial geometry. A cylindrical capacitor or coaxial line, for example, can be shorted at one end by a spark gap to obtain large amplitude oscillations at very high frequencies. A problem remains, however, in delivering the RF power to a load or radiator without appreciably increasing the inductance of the device.

In 1919 the problem was partially solved in an invention by C. S. Franklin,² a co-worker of Marconi. Franklin's device differs from a section of coaxial line in that the outer conductor is folded over on itself so that current, during discharge, must flow on the outer surface of the outer conductor, as shown by arrows in Fig. 11. The current on the outer cylinder will radiate directly; or at longer wavelengths, current can be coupled to nearby parallel conductors.

The folded geometry of Franklin's device precludes the use of multiple modules in cascade; consequently, power input can be increased only by making a single unit longer, a procedure that lowers the operating frequency. In order to cascade many modules in a coaxial geometry we discard Franklin's second outer cylinder, arrange the storage capacitors in a straight line with spark gaps interspersed as in a ring transmitter, and complete the circuit through a low-inductance cylindrical conductor that encloses the line of capacitors. The problem of coupling the energy out

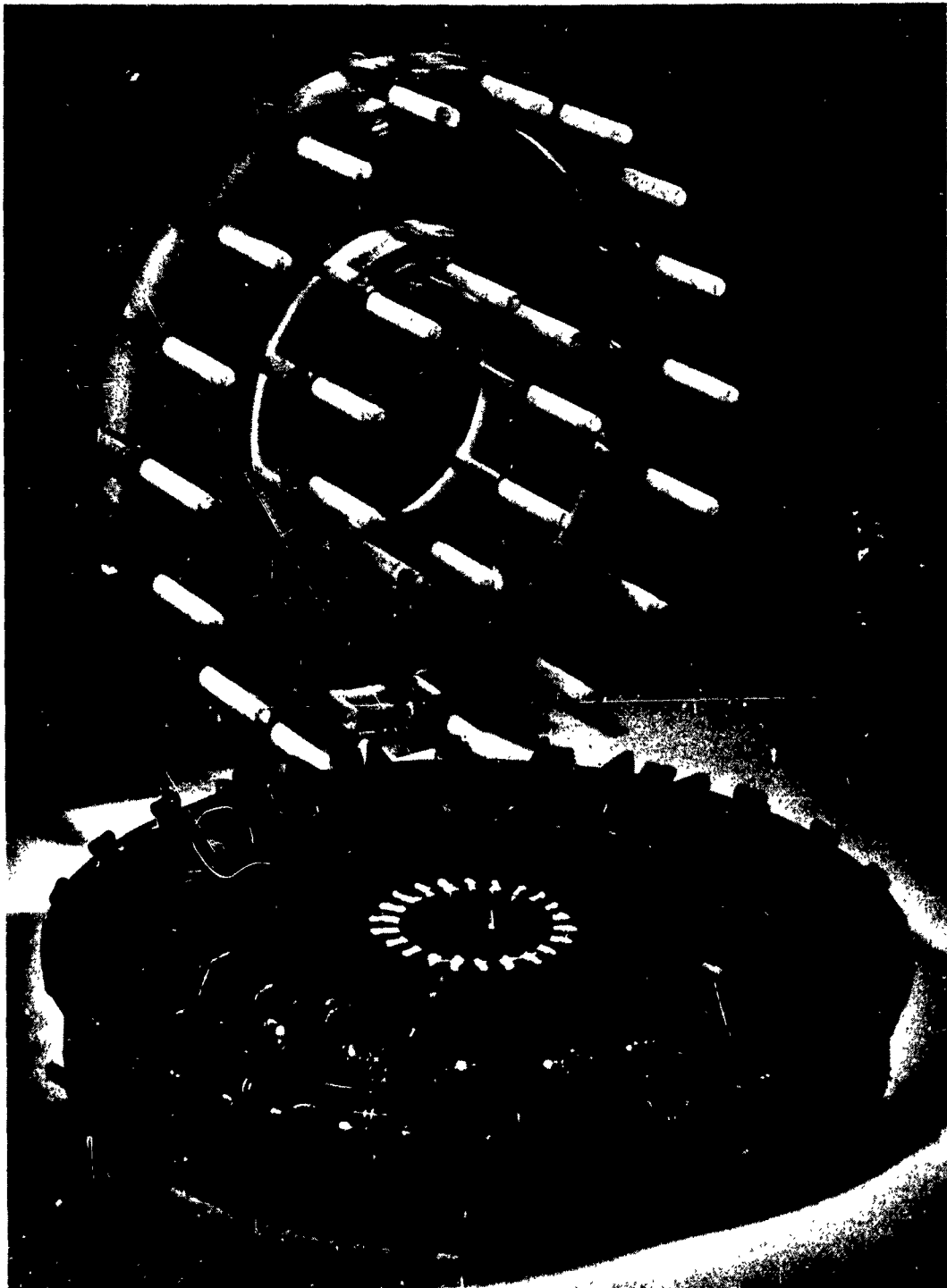


FIG. 10 150 MHz RING TRANSMITTER

The entire ring can be pressurized in the Lucite case.

Auxiliary trigger electrodes are connected to strip lines radiating from the center.

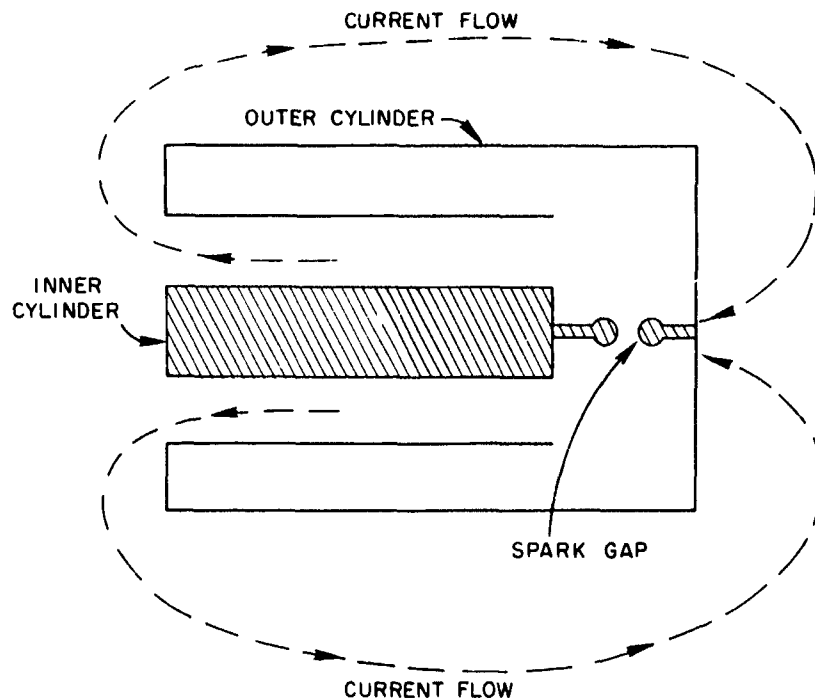


FIG. 11 SIMPLIFIED SKETCH OF FRANKLIN'S INVENTION FOR GENERATING HF RADIO ENERGY

of the closed cylinder can be solved by methods other than Franklin's. The arrangement of capacitors and spark gaps is shown schematically in Fig. 12.

The coaxial generator described above can be thought of as a shielded, loaded, hertzian oscillator in which spark gaps allow the use of the Marx generator technique of charging in parallel and discharging in series. Initially the capacitors are charged to operating potential; then the spark gaps are discharged and the stored energy generates a current in the inner conductor, the return path being the outer conductor or cylinder. If the capacitors, spark gaps, and connections are arranged in the form of an inner cylinder, the inductance of the return path can be made very small by making the diameter of the inner conductor almost as large as the diameter of the outer cylinder. Very high frequencies can be achieved even if the series capacitances are quite large. For example, we have tested a working model capable of supplying 1 to 5 MW of peak power at 20 MHz. The device is only 1.3 m long and uses 10 storage capacitors of 1500 pF each.

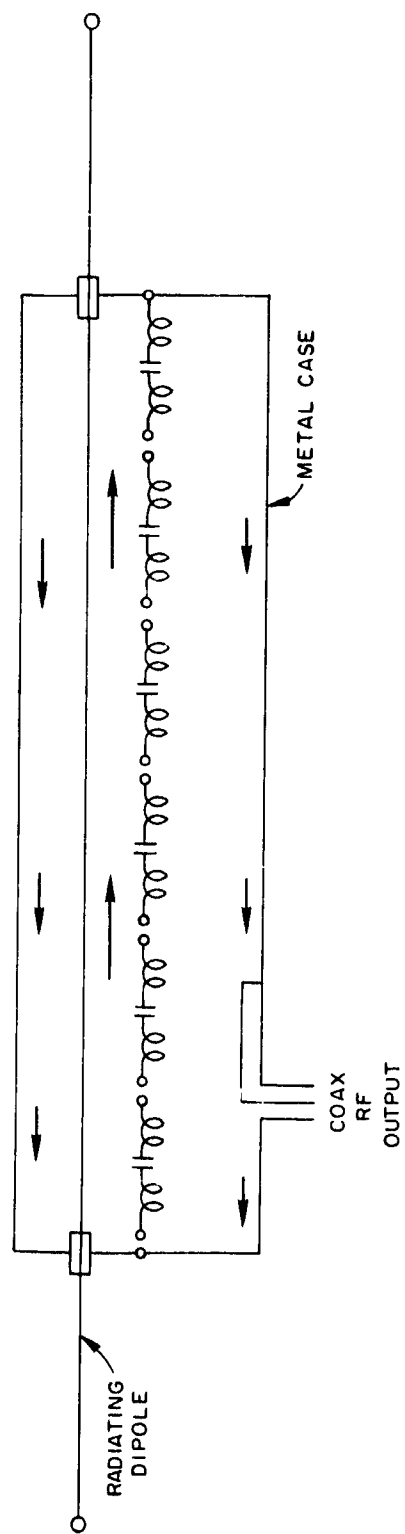


FIG. 12 SCHEMATIC DRAWING OF A MEANS OF GENERATING HIGH-POWER UHF RADIO PULSES

This model, which is shown in Fig. 13, has about the same power and frequency capabilities as the spark-ring transmitter 4 m in diameter and having 67 capacitors, each of 70 pF capacitance; thus, the cylindrical oscillator is a much more compact device. As a further example, a 90 MHz cylindrical generator was constructed that is capable of 1/2 MW peak power and is only 1 m long (Fig. 14). Since there is no limit to the length of these devices--other than practicality--it may be possible to build generators capable of hundreds of megawatts peak power.

Radio energy can be obtained from these devices by coupling to transmission lines or by modifying the cylinder to permit direct radiation. In one method a long, conducting rod is placed in an off-axis position alongside and parallel to the center conductor. The rod extends through holes in the conducting plates at either end of the outer cylinder and projects about 1/8 of a wavelength beyond both ends of the outer cylinder. The rod is insulated from the inner conductor and outer cylinder. Together with the outer cylinder, the projecting ends of the rod form an efficient halfwave dipole radiator (Fig. 14). Another method is to cut an asymmetrical slot radiator in the outer cylinder. This technique was

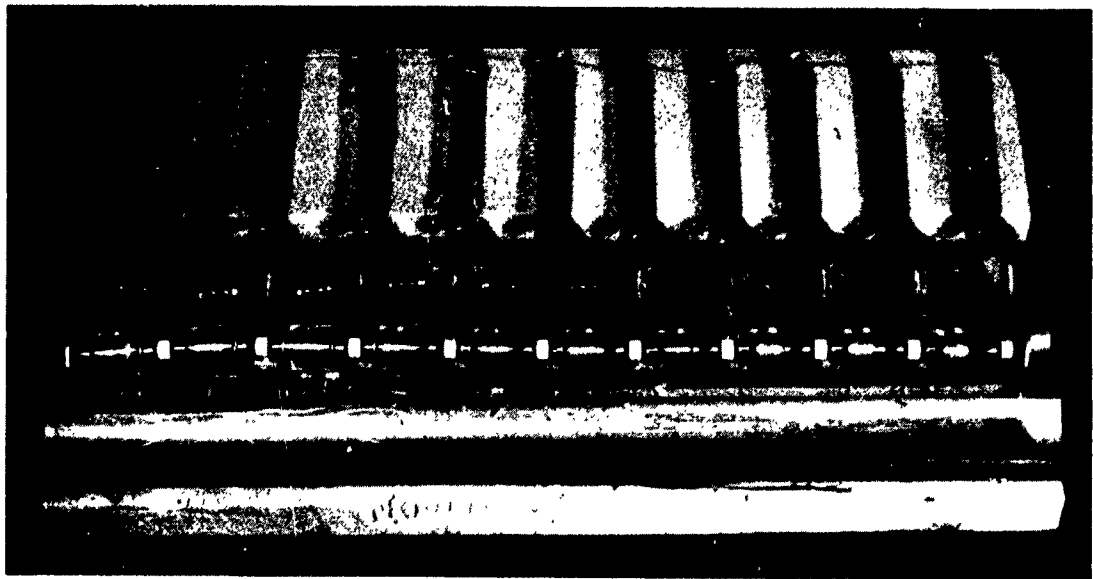


FIG. 13 20 MHz CYLINDRICAL GENERATOR
Half of the outer cylinder has been removed to show the storage capacitors, which are interconnected by pressurized spark gaps.

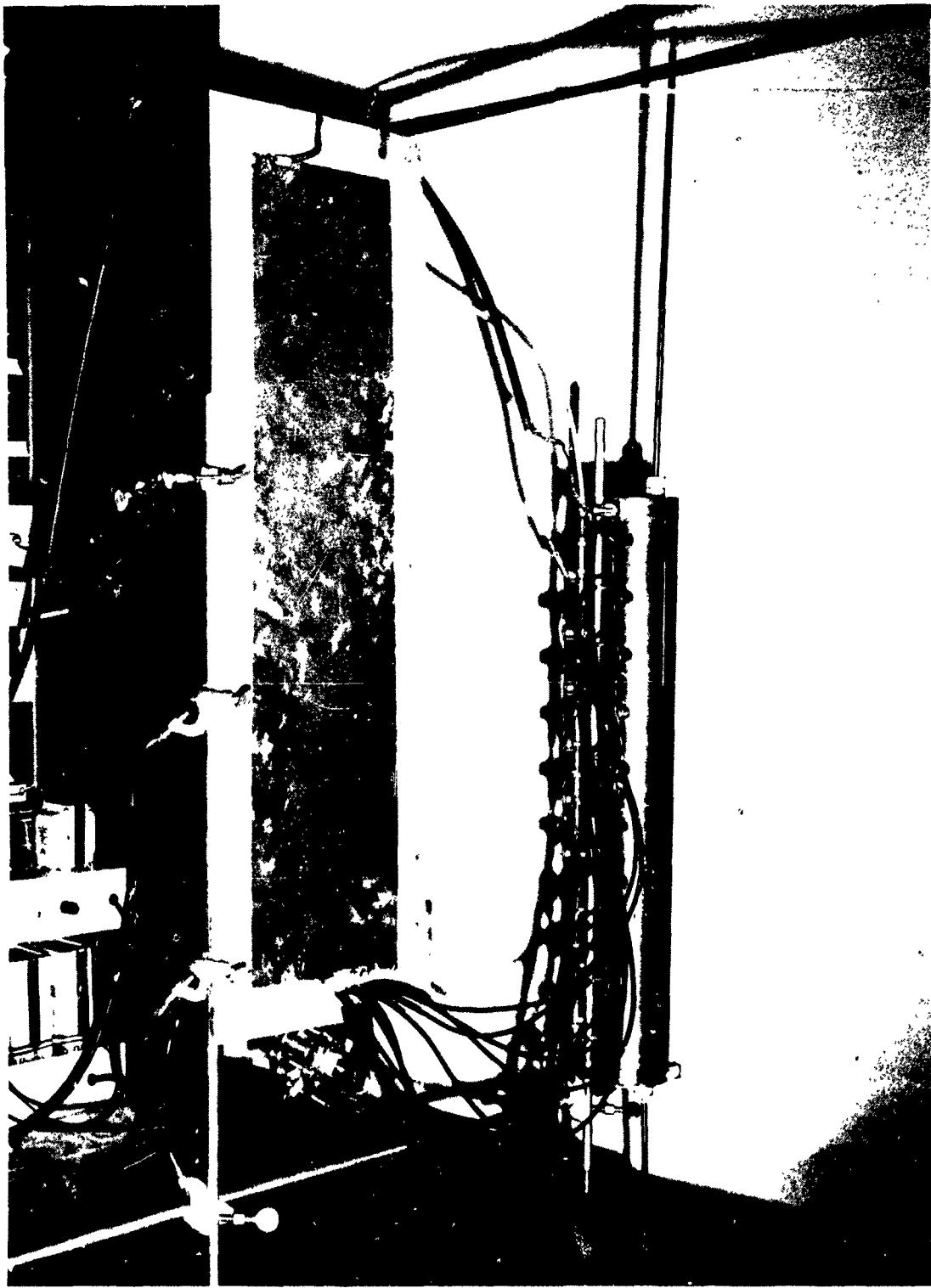


FIG. 14 90 MHz CYLINDRICAL GENERATOR WITH DIPOLE RADIATOR
Trigger cables are connected to a charged strip line
through a pressurized spark gap.

used successfully in the 100 MHz generator shown in Fig. 15. Because of insulation design error, this model had to be filled with paraffin before it could be operated at design voltage. In operation it radiated 16 percent of the stored energy at a frequency of 103 MHz. Bandwidth was approximately equal to the reciprocal of the pulse length.

We can use the 90 MHz working model to exemplify the design procedure. The inductance per meter can be computed from the formula for the inductance of a coaxial transmission line, $L = (138/3)(10^{-2}) \log_{10} (D/d) \mu\text{H}$ per meter. Since the outer and inner diameters are 9.83 and 3.18 cm and the device is 1 m long, the total inductance is 0.226 μH . There are 10 capacitors of 150 pF capacitance; thus, the total series capacitance is 1500 pF. This series capacitance tunes the inductance to a resonant or operating frequency, $f = 1/2\pi(LC)^{1/2} = 86.3 \text{ MHz}$. In actual operation the resonant frequency was 90 MHz. The capacitors were charged to about

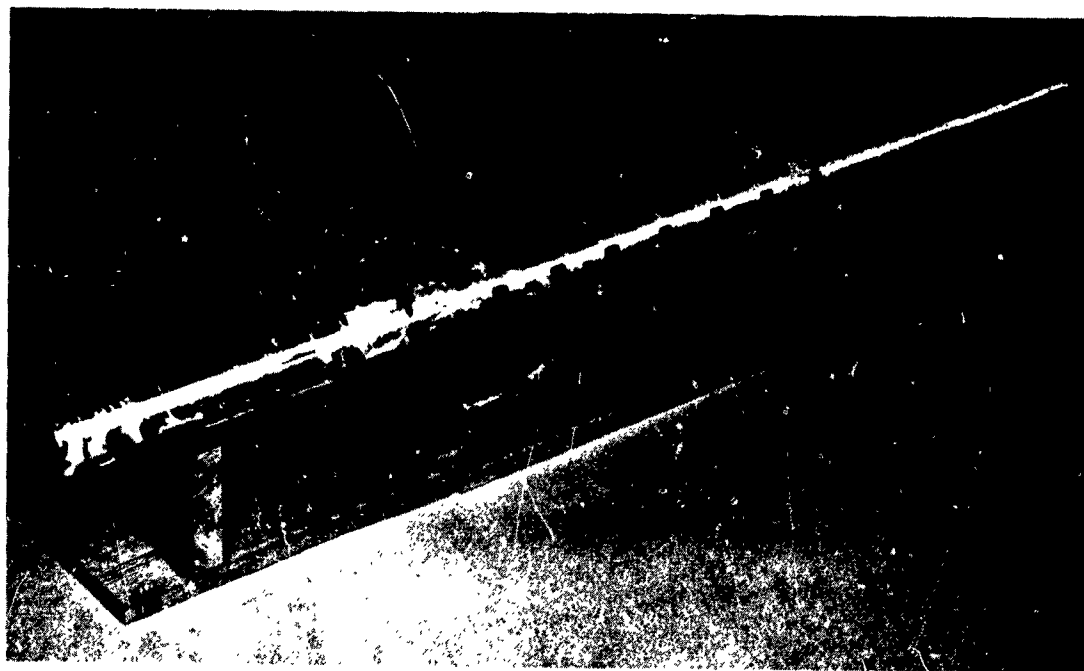


FIG. 15 PHOTOGRAPH OF A 100 MHz CYLINDRICAL GENERATOR WITH AN ASYMMETRICAL SLOT RADIATOR CUT PARALLEL TO THE AXIS. Charging resistors and trigger cables can be seen at the front and behind the cylinder.

16 kV; thus, the total stored energy per pulse is $U = 1/2CV^2 = 0.192 \text{ J}$. The length to half-power amplitude of the radiated pulse was about 40 ns; thus, the theoretical peak power is about $0.192 \text{ J}/40 \text{ ns}$, or 4.80 MW. By measuring the received power at a distant point, we determined that the peak power actually radiated was about 0.46 MW, which gives an efficiency of about 10 percent.

IV INSTRUMENTATION AND TESTING

The 23 MHz ring transmitter (Figs. 2, 3, 7, and 16) was used in many experiments and tests. In Fig. 16 it is shown with a secondary, parasitic, tuned magnetic dipole. It was demonstrated, as originally proposed by Landecker, that the secondary element could be used to increase pulse length and modify pulse shape.

When the 23 MHz ring was pressurized, but not fitted with a trigger system, its power output was measured at about 140 kW at an operating voltage of 18 kV, and the pulse shape was as shown in Fig. 17. Since power is proportional to the square of the charging voltage, an increase to the design level of 50 kV should result in an output of about 1.1 MW. Figure 18 shows some clutter echoes obtained from Black Mountain and the coastal foothills behind Stanford University. These echoes were obtained with the ring gaps pressurized to 60 psi (about 4 atmospheres) of nitrogen but without a trigger system. They are some two orders of magnitude larger than echoes previously obtained from the same target with unpressurized air gaps and a higher charging voltage.

At a later time, when the ring has been fitted with a trigger system, the measurements were repeated at 20 kV operating voltage and the measured output was 1 MW with a pulse as shown in Fig. 8. The shortening of the pulse is a result of insulation deterioration in the charging resistors and increased corona losses, problems which were recognized only near the end of the project.

A portion of one of the trigger systems used on the 23 MHz ring is shown in Fig. 19. The pressurized main spark gap shown in the figure was one of 67 which were connected in parallel to a central thyratron. Originally, a central pressurized spark chamber was built, from which the 67 trigger cables extended radially to the 67 UV gaps. This arrangement provided triggering of the ring from an external trigger pulse, but

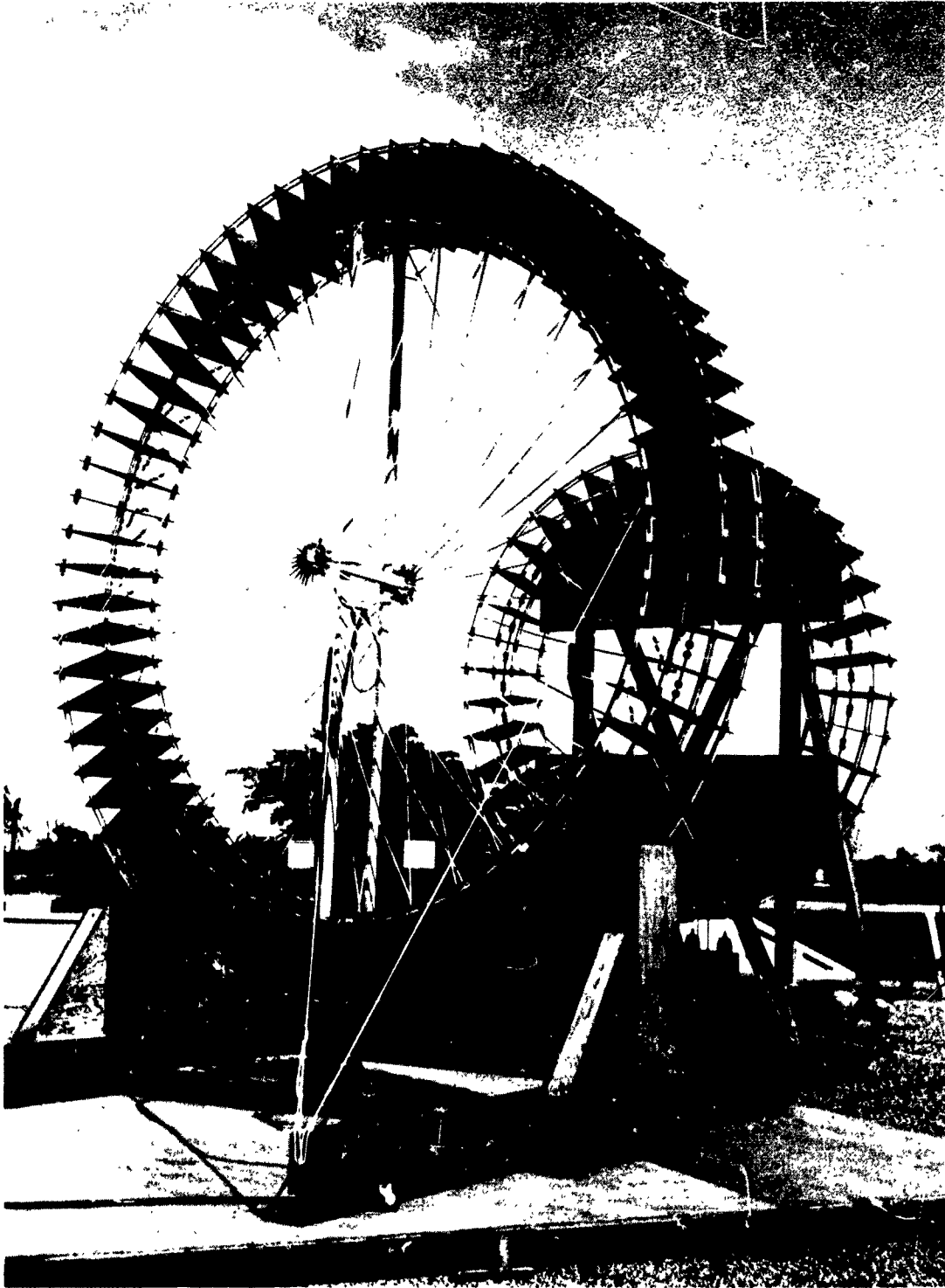


FIG. 16 EARLY MODEL OF THE RING TRANSMITTER AND A SHORTED, PARASITIC, SECONDARY RING

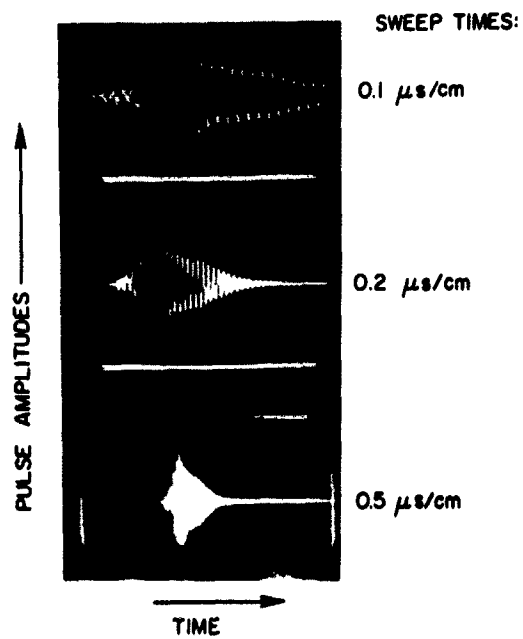


FIG. 17 PULSE WAVEFORM FROM THE PRESSURIZED 23 MHz RING TRANSMITTER

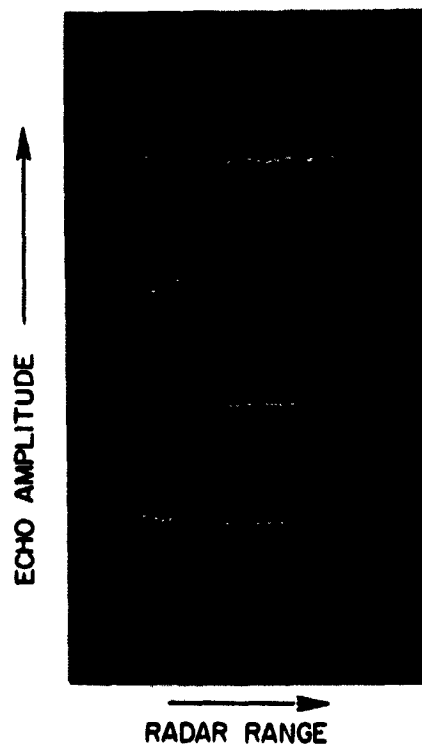


FIG. 18 A-SCOPE PRESENTATION OF CLUTTER ECHOES FROM THE 23 MHz TRANSMITTER

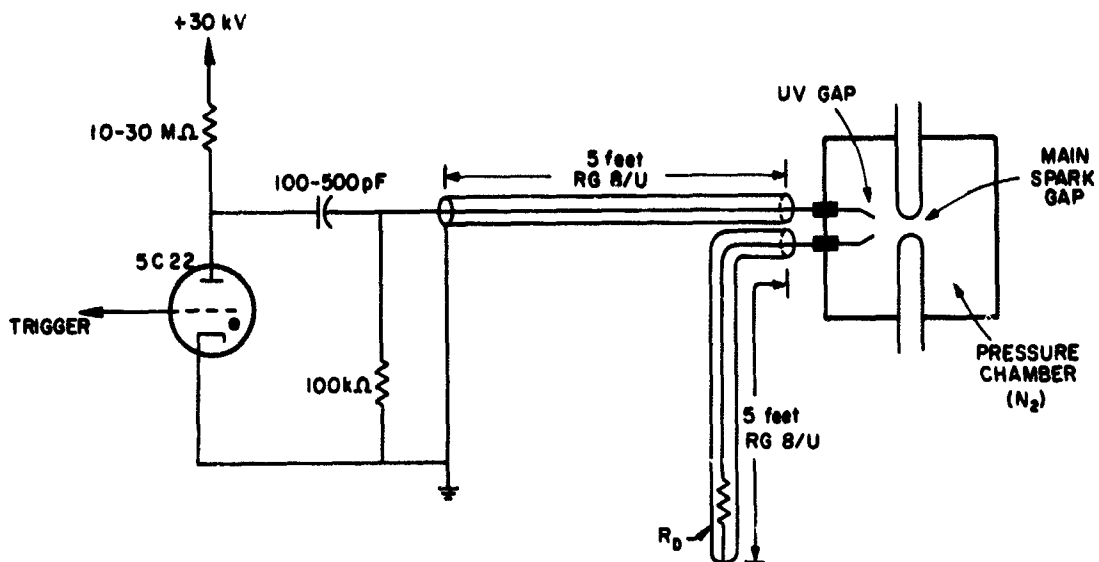


FIG. 19 A PORTION OF THE FAST-PULSE ULTRAVIOLET TRIGGERING CIRCUIT

not without a high degree of jitter since the central chamber contained a multiplicity of spark gaps activated by a single spark in the center. The central chamber was later replaced by a commercially available triggered spark gap called a "trigatron." While jitter time below 20 or 30 ns was not expected, according to the manufacturer, there was considerable advantage in having a single high-current discharge for energizing all 67 trigger leads. The trigatron was driven by a 5C22 thyatron, and the thyatron, in turn, was driven by pulse amplifiers and a commercial high-speed pulse generator having an output pulse of 200 V with a rise time of 15 ns.

Figure 20 is an oscillogram of superimposed traces of the triggering pulse. The PRF was about 1 pps. From the photograph it can be seen that the pulse-to-pulse jitter is about 3-5 ns. In order to be sure that only overall jitter time was measured, the oscilloscope sampling probe was connected to a load resistor (R_D in Fig. 19) so that no signal could arrive at the oscilloscope until after the UV gap had discharged.

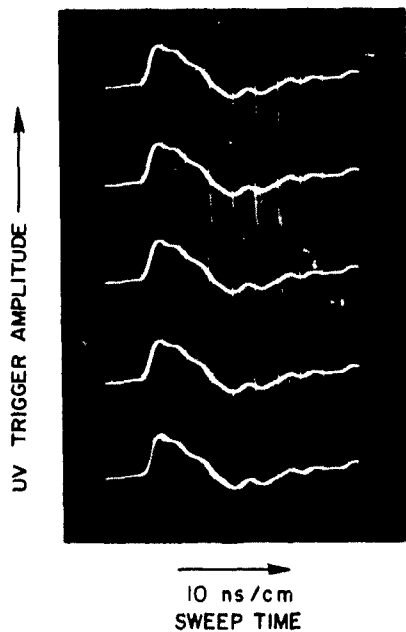


FIG. 20 OSCILLOGRAM OF SUPERIMPOSED PULSES FROM THE TRIGGERING SPARK GAPS

With the experimental arrangements described above, it was found that the RF pulse could be triggered with an accuracy of 3 to 5 ns, provided the main gap voltage was adjusted to within a few percent of the self-firing voltage. Study of the jitter time at various stages along the triggering chain indicated that the main source of jitter was the trigatron. When the thyatron was heavily and rapidly over-voltaged, it could be made to fire a single UV gap with a jitter of only 1 to 3 ns.

At a later time we found it was possible to achieve triggering with fractional-nanosecond jitter; however, a pair of 6 MHz ring transmitters were built to test the

joining of RF pulses with the less accurate triggering system described above. A jitter of 3 to 5 ns is sufficiently accurate for phase coherency at 6 MHz; in addition, the lower frequency permits ionospheric echoes and a comparison of performance with conventional sounders. A schematic of the trigger system built for the 6 MHz rings is shown in Fig. 21.

The 6 MHz rings were small, having a diameter of 0.15λ ; consequently, the radiation resistance was only 8Ω . Each ring consisted of 20 capacitors, each of 1500 pF capacitance (Fig. 22). A third was also built with shorted gaps and used as a parasitic, tuned element for pulse stretching. In addition, a larger secondary ring was built to couple power from the driver rings and radiate it upwards. A photograph of the entire system is shown in Fig. 23. Operating at a charging voltage of 30 kV, the two driver rings develop 1 to 2 MW each and have a pulse length of 4 μ s.

The pulse from one of the 6 MHz driver rings, observed by connecting a small antenna directly to the plates of a high-speed oscilloscope located a few dozen yards away from the ring, is shown in Fig. 24(a). The effect of adding the tuned secondary circuit to a driver ring is shown in Fig. 24(b). The secondary was coupled to the primary circuit, and since it had a higher operating Q than the primary, the energy exchange with the primary lengthened the total pulse. The effect of the high-Q secondary circuit is shown more clearly in Fig. 25, a photograph taken at a slower sweep speed. Careful adjustment of coupling coefficient and secondary circuit tuning lengthens the radiated pulse by a factor of 5 to 10. Although the average power during the pulse is reduced proportionally, a longer pulse is sometimes desired in radar work.

Pulse-to-pulse jitter in the RF signal from one of the 6 MHz driver rings is shown in Fig. 26. By triggering the oscilloscope with a master pulse generator sequential RF pulses, one second apart, were superimposed for this photograph. Jitter times of 3 to 5 ns were obtained, and stable performance was achieved by adjusting gas pressure, gap settings, and applied voltages.

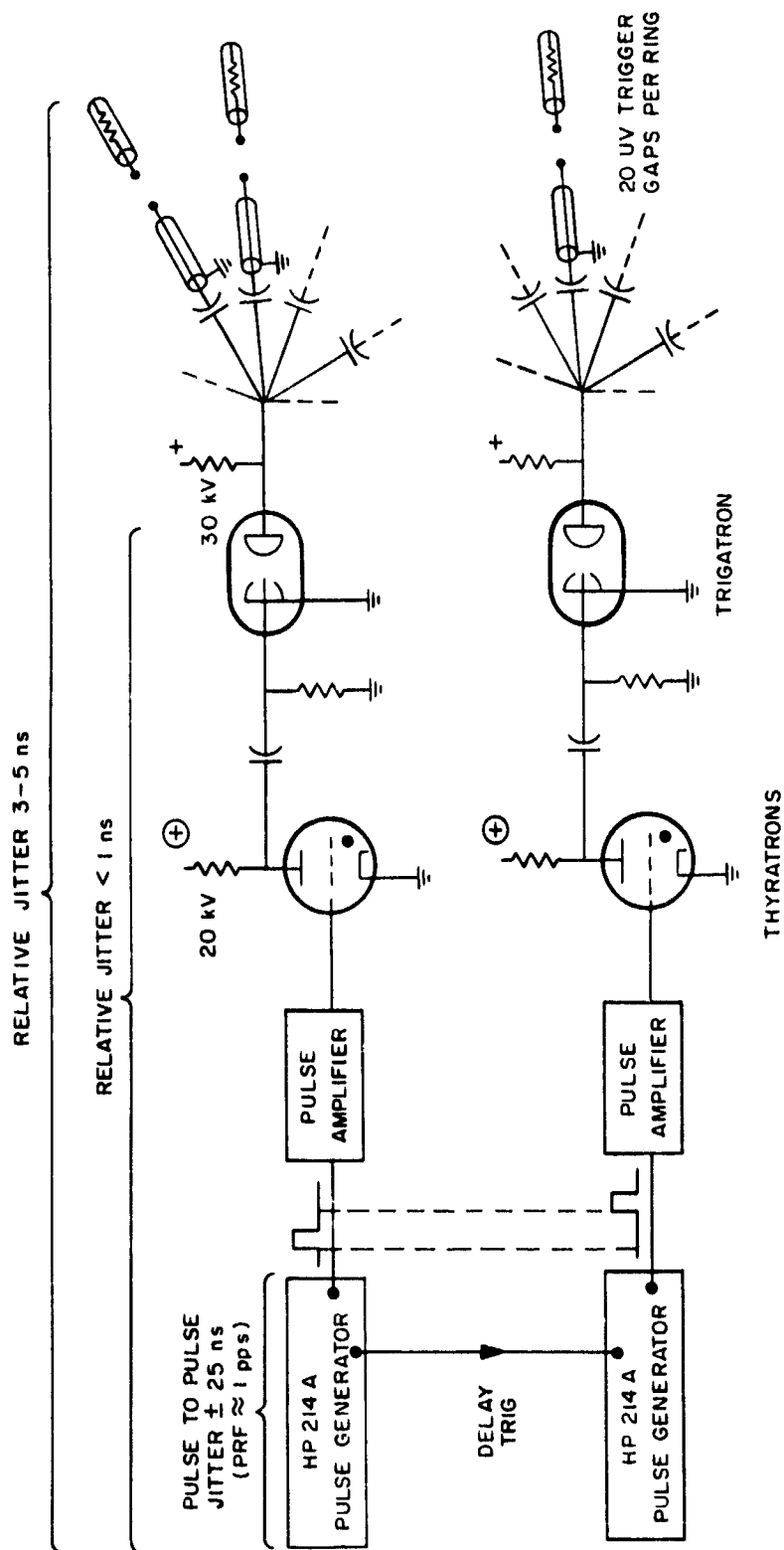


FIG. 21 SCHEMATIC DIAGRAM OF THE DELAYED-PULSE TRIGGERING CIRCUIT USED WITH THE 6 MHz RING TRANSMITTERS



FIG. 22 6 MHz SPARK-RING TRANSMITTER

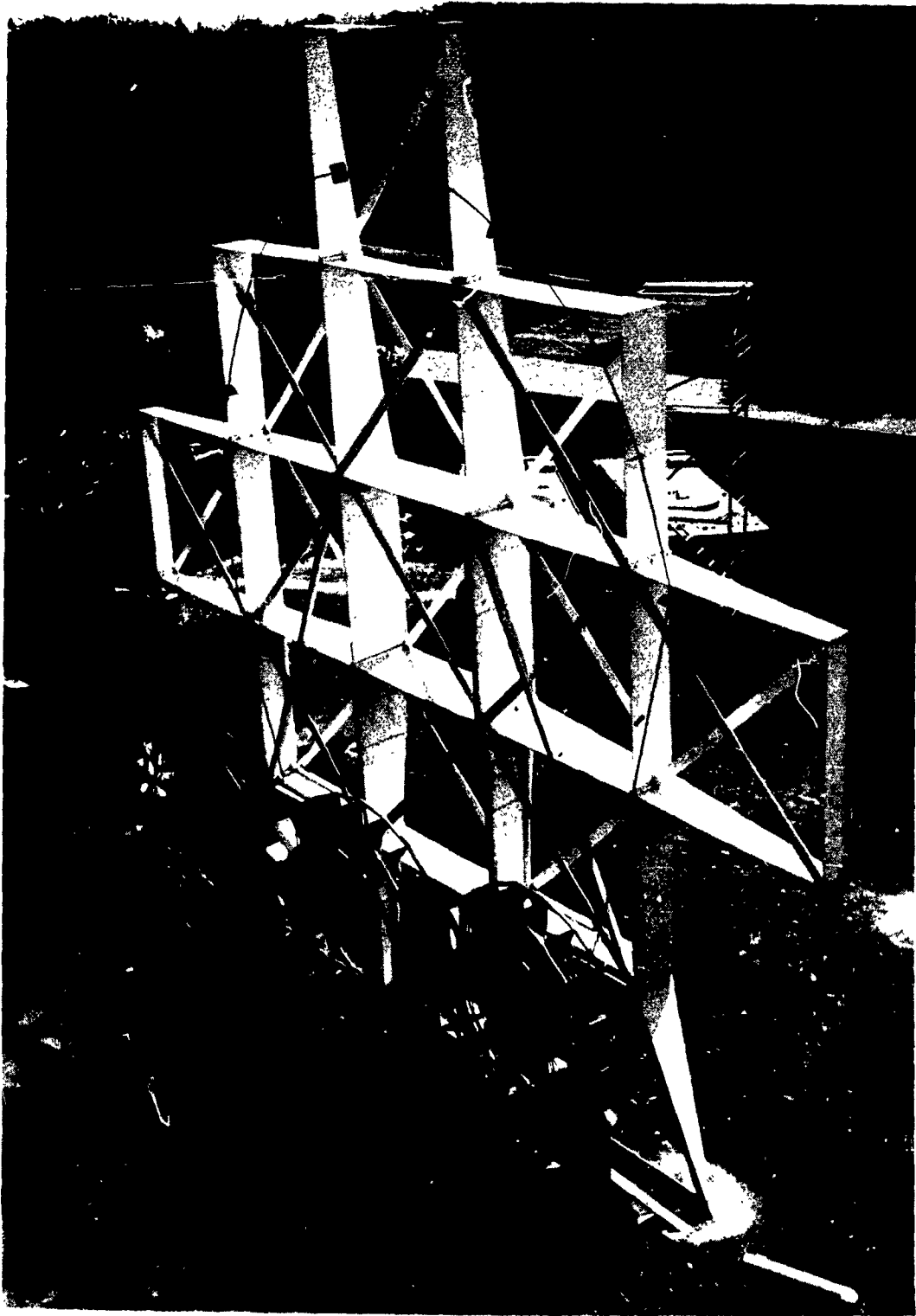


FIG. 23 TWO DRIVER (Active) 6 MHz RING TRANSMITTERS COUPLED TO A SHORTED, PARASITIC 6 MHz RING AND A FOURTH, LARGER TUNED RING

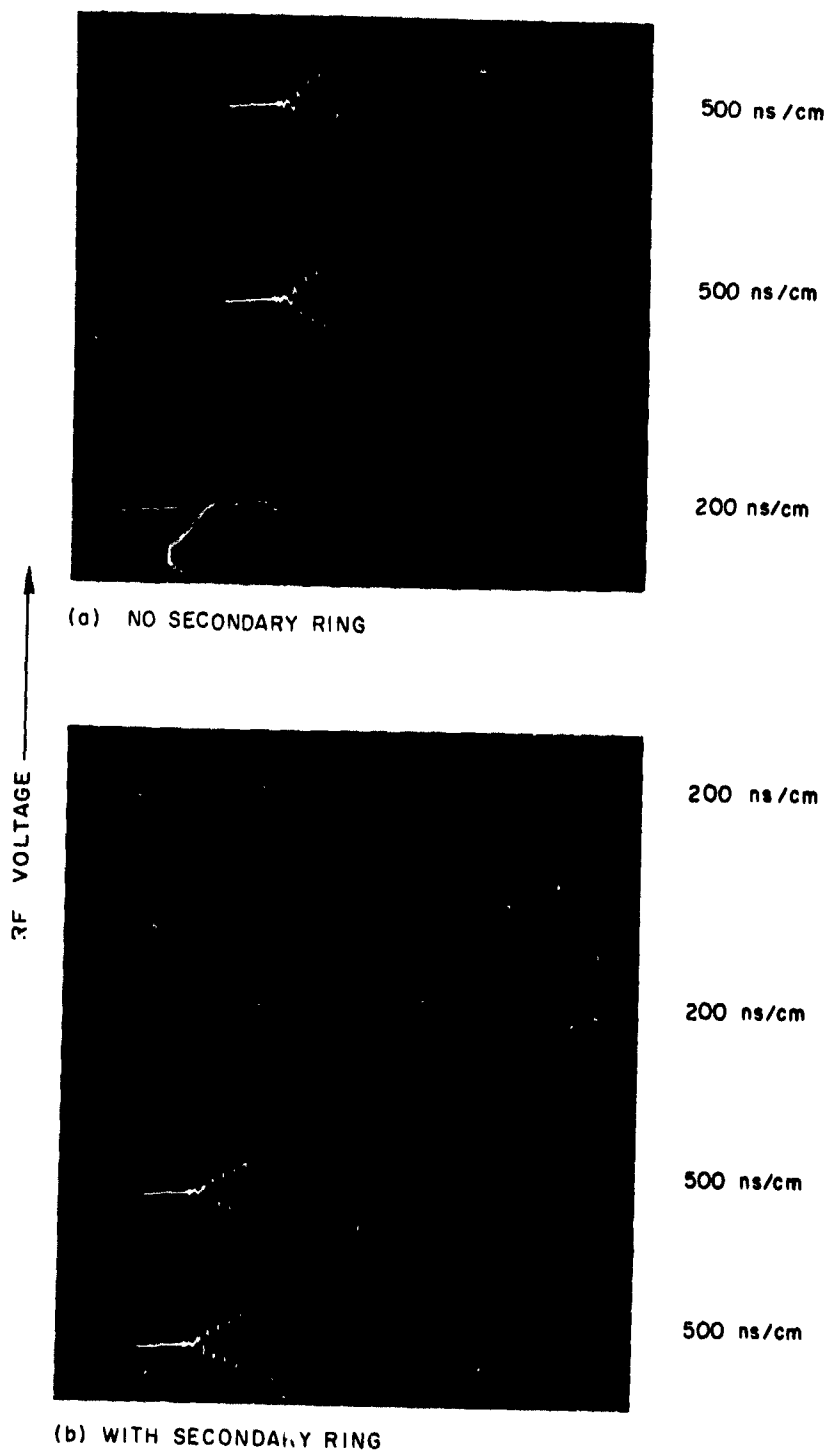
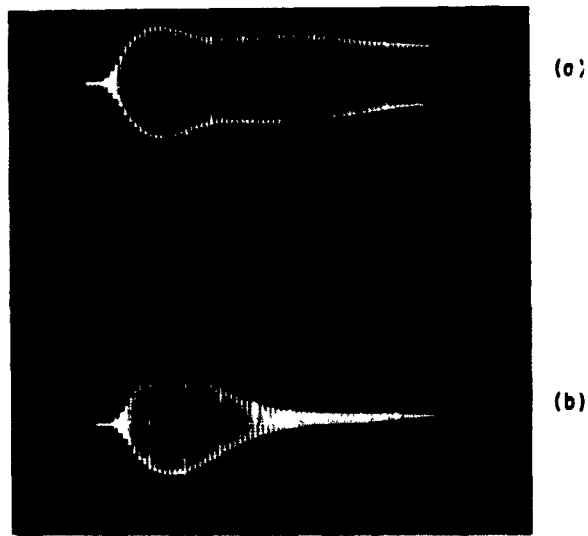
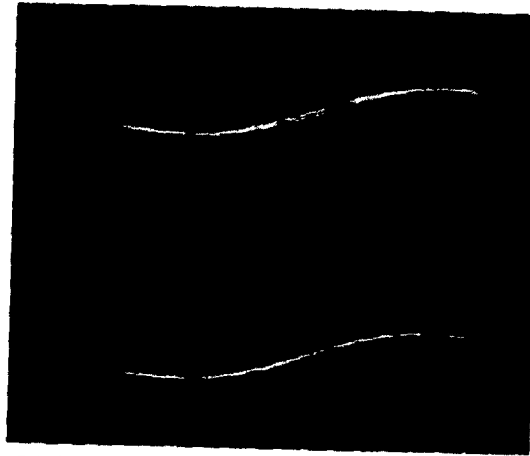


FIG. 24 RF PULSES FROM A 6 MHz RING TRANSMITTER
 (a) Without a Secondary Ring
 (b) With a Secondary, Parasitic Ring

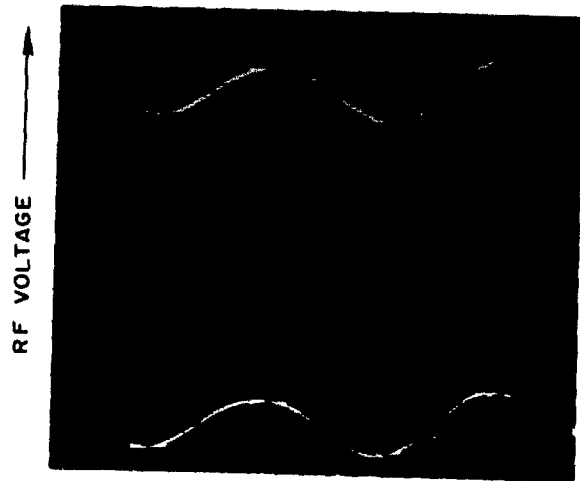


SWEEP
1 μ s/cm

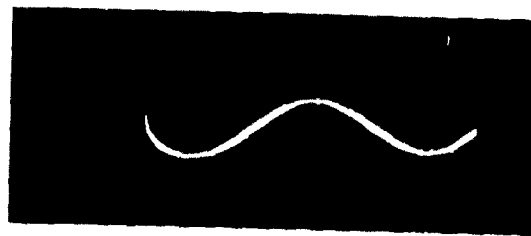
FIG. 25 RF PULSES FROM A 6 MHz RING TRANSMITTER,
SHOWING THE EFFECT OF COUPLING
A HIGH-Q, TUNED, SECONDARY RING
TO THE DRIVER RING



SWEEP TIME 10 ns/cm →



RF VOLTAGE ↑



SWEEP TIME 20 ns/cm →

FIG. 26 6 MHz RADIATED SIGNAL,
SHOWING PULSE-TO-PULSE JITTER
(PRF \approx 1 pps)

The RF pulses from the two 6 MHz driver rings, triggered by the circuit shown in Fig. 21, are shown in Fig. 27. The rings were fired sequentially for this photograph. The second ring was fired slightly after the first ring, so that a double pulse was obtained as shown. With a third, parasitic ring, the double pulses in Fig. 28 were obtained. Since the second ring start time could be continuously adjusted, it was

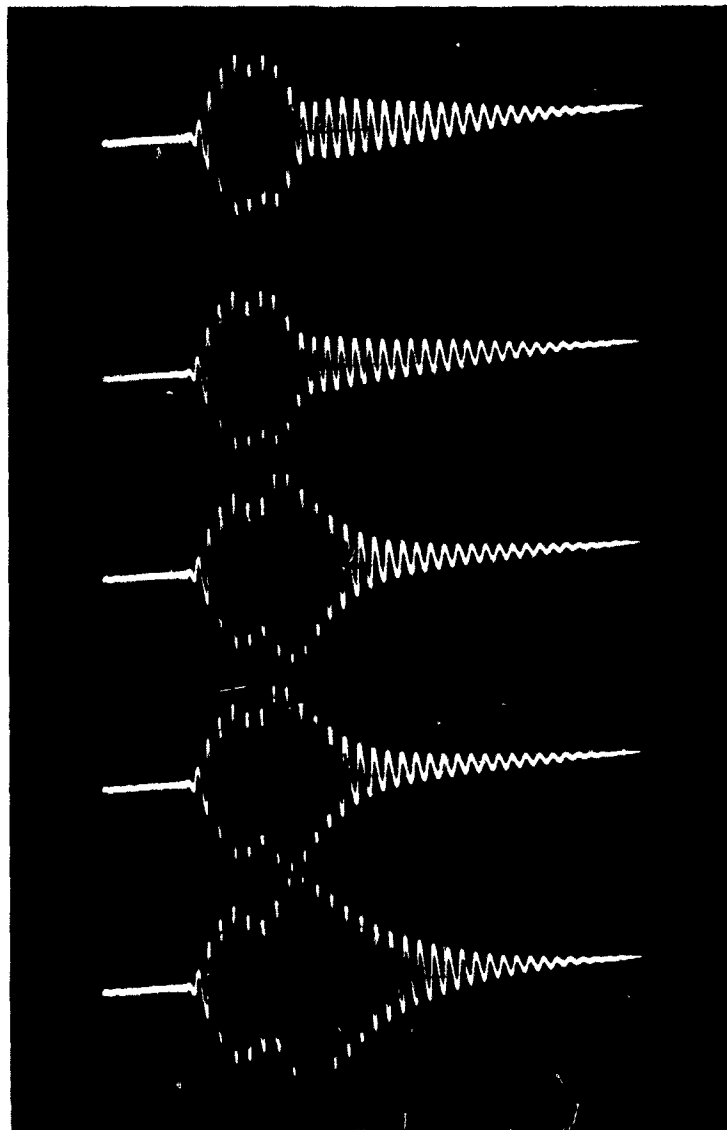
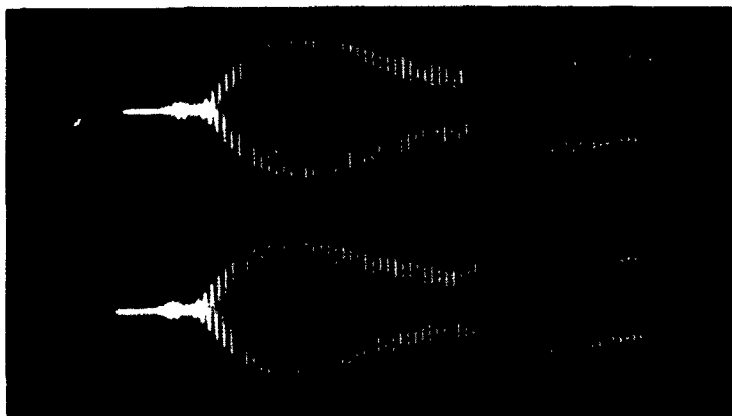


FIG. 27 COMBINED RF PULSES FROM TWO ACTIVE, 6 MHz RINGS
(No Parasitic Ring)



SWEEP SPEED
1 μ s / div

FIG. 28 COMBINED RF PULSES FROM TWO ACTIVE,
6 MHz RINGS, USING A THIRD, PARASITIC RING

found that the rings could be made to fire simultaneously, or delayed up to many microseconds. Delay adjustment was sensitive enough to permit the relative phase of the two pulses to be accurately controlled and held with a precision of 3 to 5 ns. Figure 29 shows the junction of the two pulses as the starting time of the second ring was varied with respect to the first. The fact that double pulses can be generated suggests the possibility of a CW transmitter. It is believed that a single ring can be operated at a PRF as high as 40,000 pps so that only about 10 rings would be required for a form of CW operation.

Power output of a 6 MHz ring transmitter was estimated by measuring the current induced in a nearby ring having shorted gaps. It was found that the power transferred was 1 to 2 MW at 6.6 MHz. Radar echoes from the F layer, received remotely, are shown in Fig. 30. Strength of the received echoes is consistent with the measured power. The signal from the transmitter was relatively narrow, having a bandwidth of about 200 kHz, which is approximately what is expected for a pulse length of 4 μ s. The ionosphere causes considerable dispersion in the pulses: although the transmitted pulse is only a few microseconds long, both ordinary and extraordinary return pulses are often longer than 40 μ s.

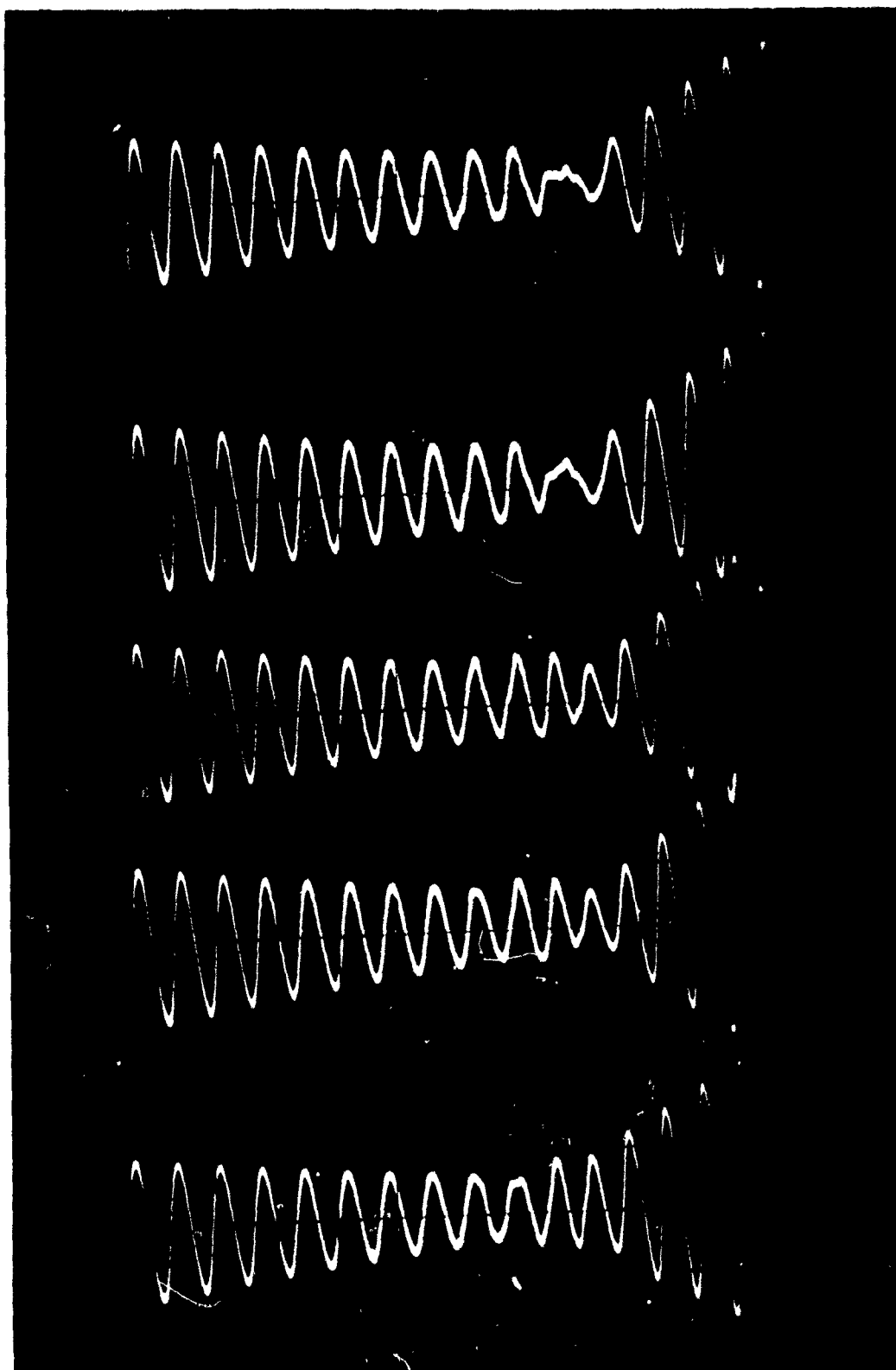


FIG. 29 JUNCTION OF PULSES FROM TWO 6 MHz RING TRANSMITTERS
Effect of varying the phase of the second pulse with respect to the first.

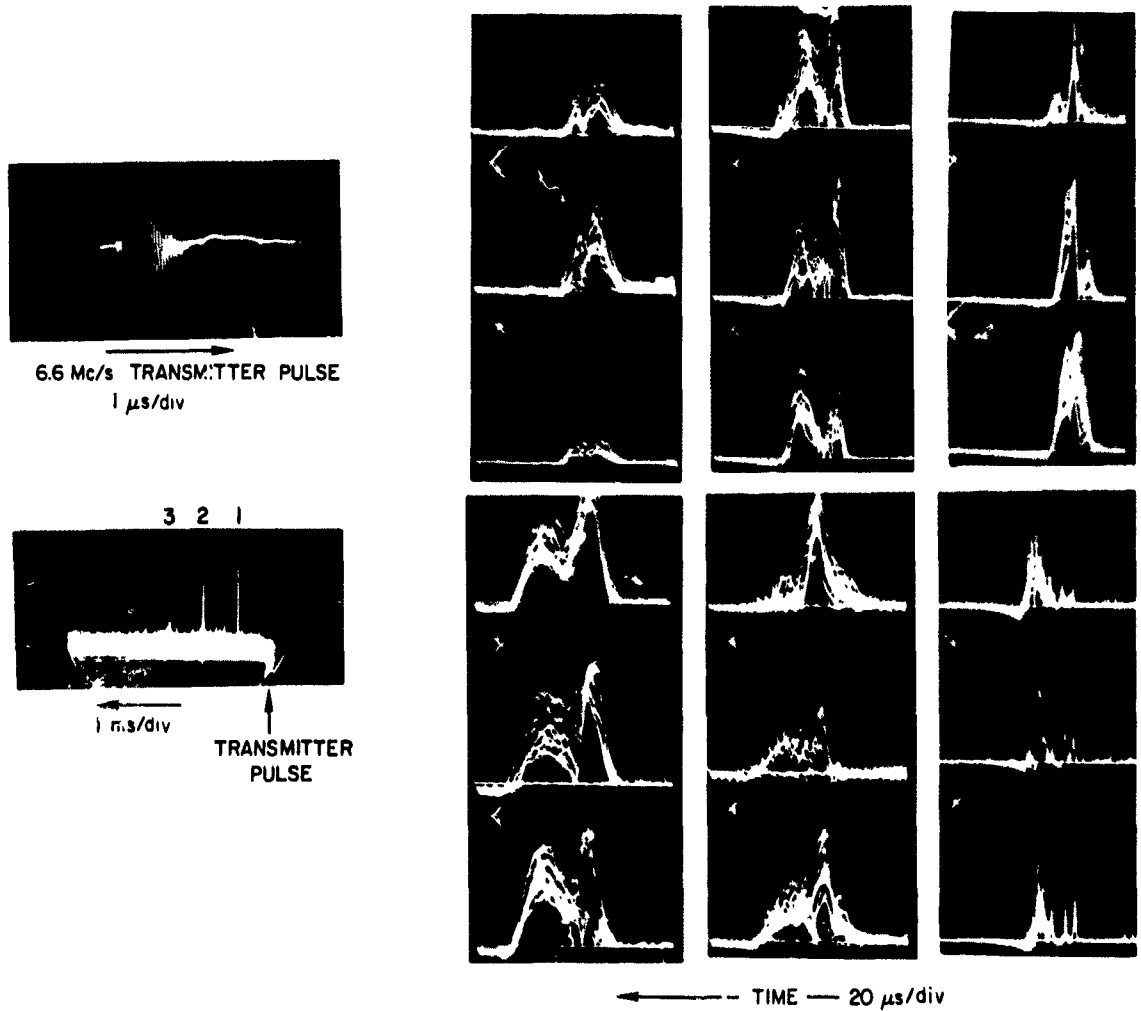


FIG. 30 F-LAYER ECHOES OBTAINED WITH THE 6.6 MHz RING TRANSMITTER SYSTEM

At the present time a complete radar system is under construction using ring transmitters at 6, 12, and 24 MHz. Some of the system parameters are given in Table II. The 12 MHz transmitter is shown mounted on a radome platform in Fig. 31. All three transmitters are shown under radomes in Fig. 32. The trailer shown in the left side of the photograph contains the radar receivers and power supplies; in the right side of the photograph there are arrays of parasitic elements which will be coupled to the ring transmitters to provide directivity.

Table II

RING-TRANSMITTER RADAR
SYSTEM PARAMETERS

Frequency	Pulse Width	Power	PRF
6.6 MHz	4 μ s	1-5 MW	0-100 pps
12.0 MHz	2 μ s	1-5 MW	0-100 pps
23.0 MHz	1 μ s	1-5 MW	0-100 pps



FIG. 31 12 MHz RING TRANSMITTER SHOWN MOUNTED ON RADOME PLATFORM



FIG. 32 RING-TRANSMITTER RADAR SYSTEM AT 6, 12, AND 24 MHz
Transmitters are protected by the three radomes; receivers and power
supplies are in the van at left. On the right are arrays of parasitic
elements which will be used to increase the directivity of the transmitters.

V CONCLUSION

In comparing contemporary work with the spark-transmitter technology of sixty or even twenty years ago, we believe the significant differences lie in dielectric materials and spark-discharge technique. While inventiveness is necessary for the application of knowledge, the extent of the advance will probably be limited by dielectric strength and spark behavior.

The ultimate high-frequency limit of practical transmitters is determined by a characteristic time, τ , required for the discharge of stored energy. If S is a characteristic length of a capacitor--say an average distance through which energy must flow during discharge--then the characteristic time will be $\tau = \eta S/C$, where η is the refractive index, or square root of the dielectric constant, and C is the speed of light. The reciprocal of τ will be a measure of the ultimate frequency attainable. The energy stored is proportional to the dielectric constant: $1/2CV^2 \propto \eta^2 SV^2$. Comparing the expressions for period and energy storage, we see that there is advantage in having a high dielectric constant: energy storage increases with η^2 (the dielectric constant) while period is lengthened by only the first power of η (the square root of the dielectric constant for most materials). In the last few decades high quality, high dielectric constant zirconates and titanates have become readily available at reasonable cost.

The ultimate frequency attainable will also depend on the speed of a spark discharge, and the highest frequency at which coherence (for arrays or for pulse-Doppler radars) can be achieved will depend on controllability as well as speed of discharge. While knowledge of the ultraviolet flash antecedent to breakdown has been available since 1938,³ there does not appear to have been a conscious application of the effect until 1957.⁴ Further, the nature of the fast streamer breakdown and the conditions under which it occurs, as opposed to the slower regenerative breakdown, have been established rather slowly even though they were

proposed 25 years ago in 1940.⁵ We have not determined minimum jitter-time limits or how fast a discharge can be made to occur in high-pressure, over-voltaged, ultraviolet-triggered spark gaps. Present research has shown that control times can be a few tenths of a nanosecond or smaller. Time intervals smaller than these are difficult to measure in non-repetitive phenomena. It may be that the easiest way to determine the ultimate power-frequency capability of spark transmitters will be to build them and see if they work.

Thus far, it appears that powers of 10 to 100 MW may be possible at frequencies of 100 to 200 MHz; also, array elements and sequential pulses can be coherent at such frequencies. We have not determined the extent to which these frequencies can be increased. At lower frequencies larger powers can be achieved readily. From 1 to 50 MHz, power levels of gigawatts are reasonable.

The success achieved with spark-transmitter techniques suggests a number of types of low-cost CW or pulse transmitters which may be useful. We shall consider the following examples: a portable UHF field radar; a gigawatt HF pulse radar; a megawatt CW, HF transmitter; and a 50 MW, VLF transmitter.

A portable UHF radar could be made compactly in the form of a cylindrical transmitter. The models shown in Figs. 14 and 15 generate UHF pulses about $1/4$ to $3/4$ μ s long at power levels of $1/2$ MW, and require charging voltages of only 10 or 15 kV. Such transmitters weigh only a few pounds and are a meter or so in length. If the average power requirement is low, a battery pack would be sufficient for operation in the field. Power levels in the 0.5 to 5 MW range at single, fixed frequencies from 20 to 200 MHz are reasonable at the present time. Figure 33 is an artist's sketch of such a radar. Assuming a 1 MW peak power, a $1/2$ μ s pulse, 6-element yagi arrays for transmitter and receiver, and a frequency of 100 MHz, we find that this radar would detect a 1 m^2 target at a range of 35 km, or 40 m^2 at 100 km range.

To achieve peak pulse powers of the order of a gigawatt we could use an array of cylindrical transmitters. The array technique provides

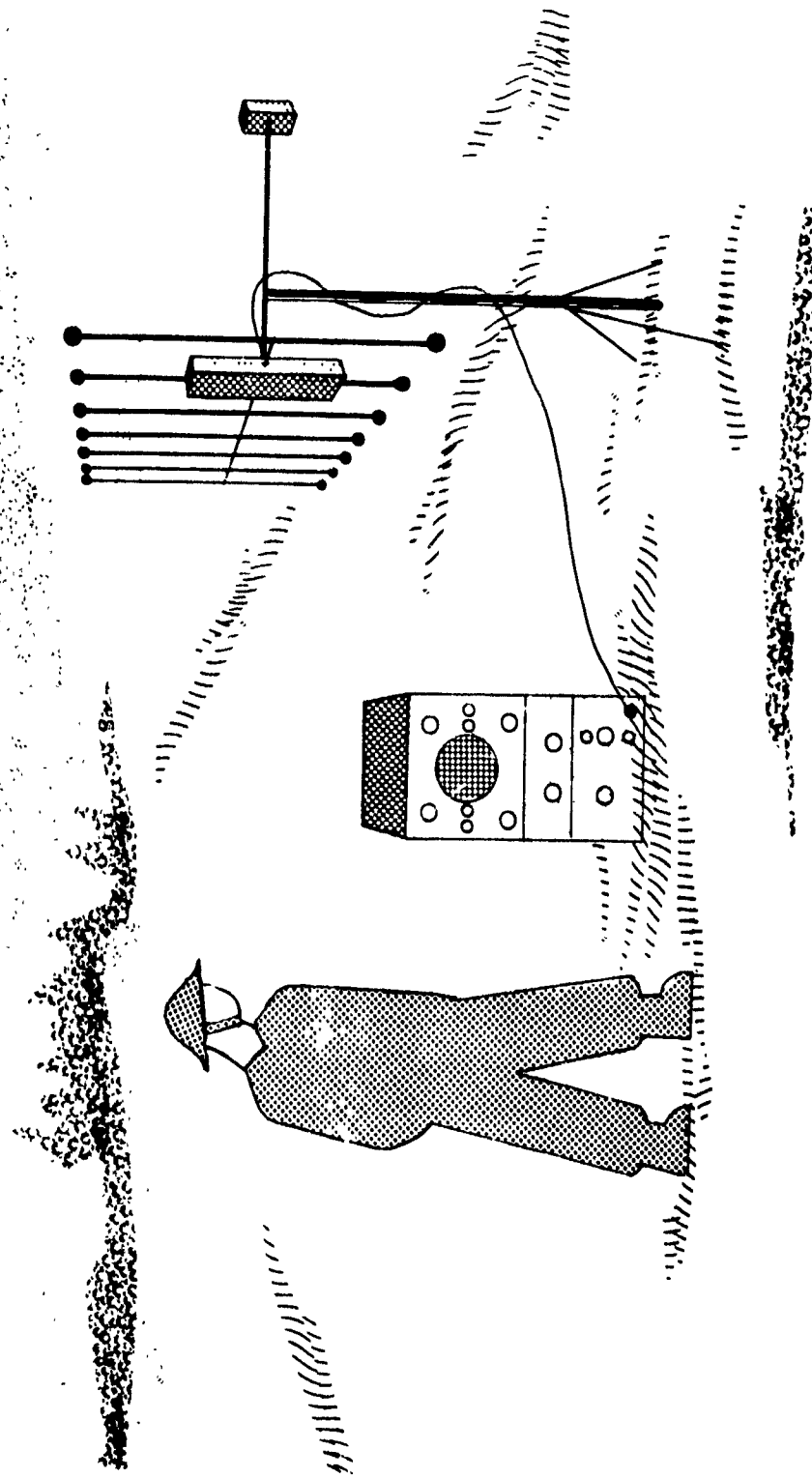


FIG. 33 ARTIST'S CONCEPTION OF A PORTABLE UHF FIELD RADAR

a large aperture with a correspondingly narrow beam, and electrical steering of the beam could be provided by phasing the triggers to each element of the array. A ten-by-ten array of 100 cylindrical transmitters would require only 10 MW per transmitter, which is easily obtainable at the present time. Transmitters about 2 m long and perhaps 15 cm in diameter would provide the required 10 MW.

To obtain CW power in the HF band we would use several ring or cylindrical generators coupled to a common high-quality secondary circuit. The individual generators would be sequentially fired with accurate time control so as to sustain CW oscillations in the secondary ring. With PRF of 20,000 pps at an RF of 20 MHz, five to ten generators would be sufficient. AM or FM modulation could be provided.

The possibility of using spark-transmitter techniques in VLF systems has been discussed previously.⁶ Figure 34 shows a sketch of the ring-transmitter technique in a VLF system. The antenna, in the form of a magnetic loop over a ground plane, has the radiation resistance and patterns shown in Figs. 35 to 37. With 200 capacitors, each 0.256 μF , and a charging voltage of 150 kV, the radiated peak power would be about 50 MW and the pulse would be approximately 1 ms long. At 30 kHz the antenna would be 400 m high and 5000 m long, giving a radiation resistance of 6 Ω . Spark-gap resistive losses of 0.1 to 0.3 Ω per gap would reduce the overall efficiency to about 8 percent. Two or more VLF loop antennas would permit phasing of the radiated signal to steer the beam (Fig. 38). Several identical loops in parallel, triggered sequentially, would permit CW operation.

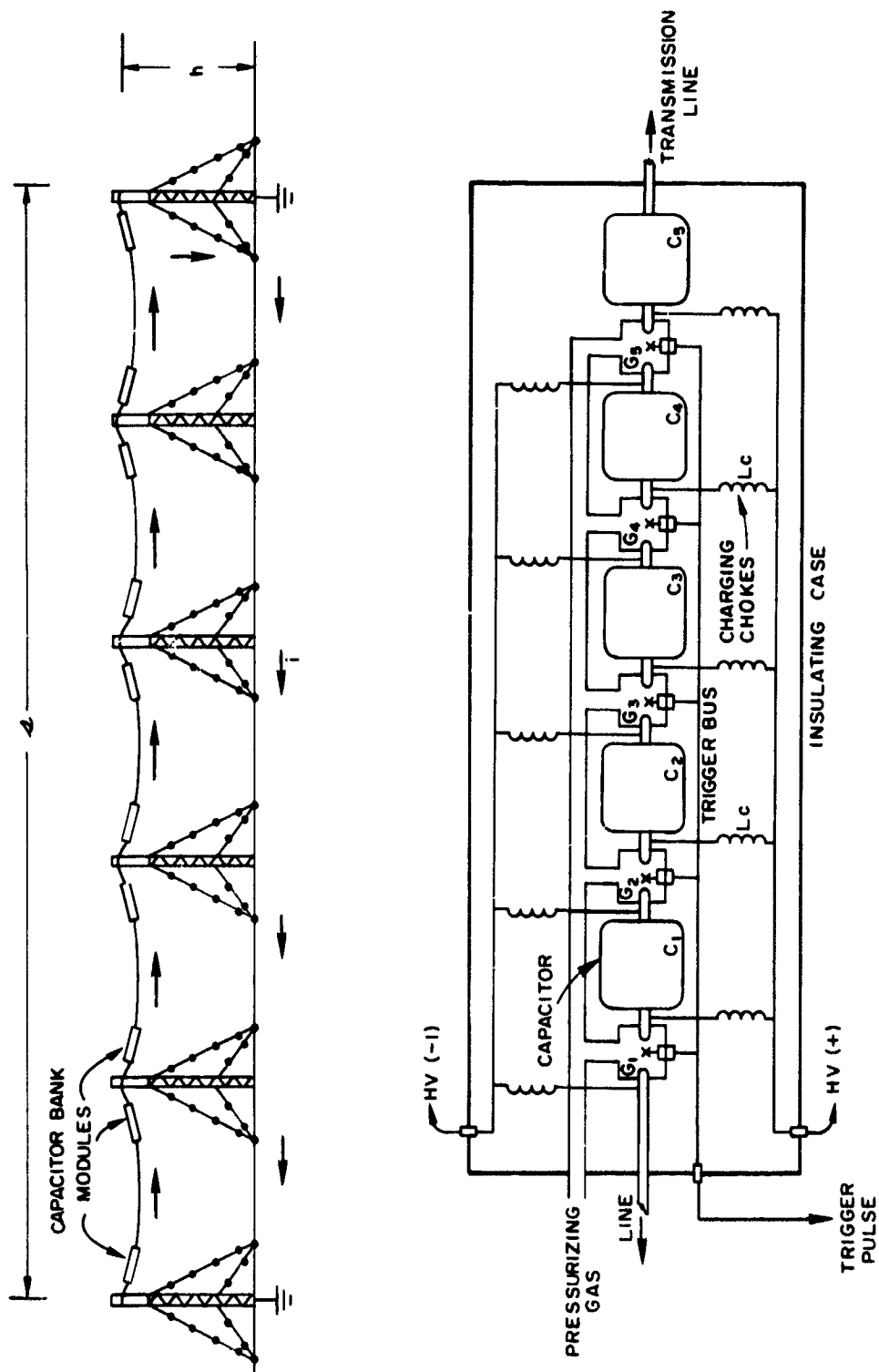


FIG. 34 PROPOSED FORM OF A 50 MW, VLF PULSE TRANSMITTER

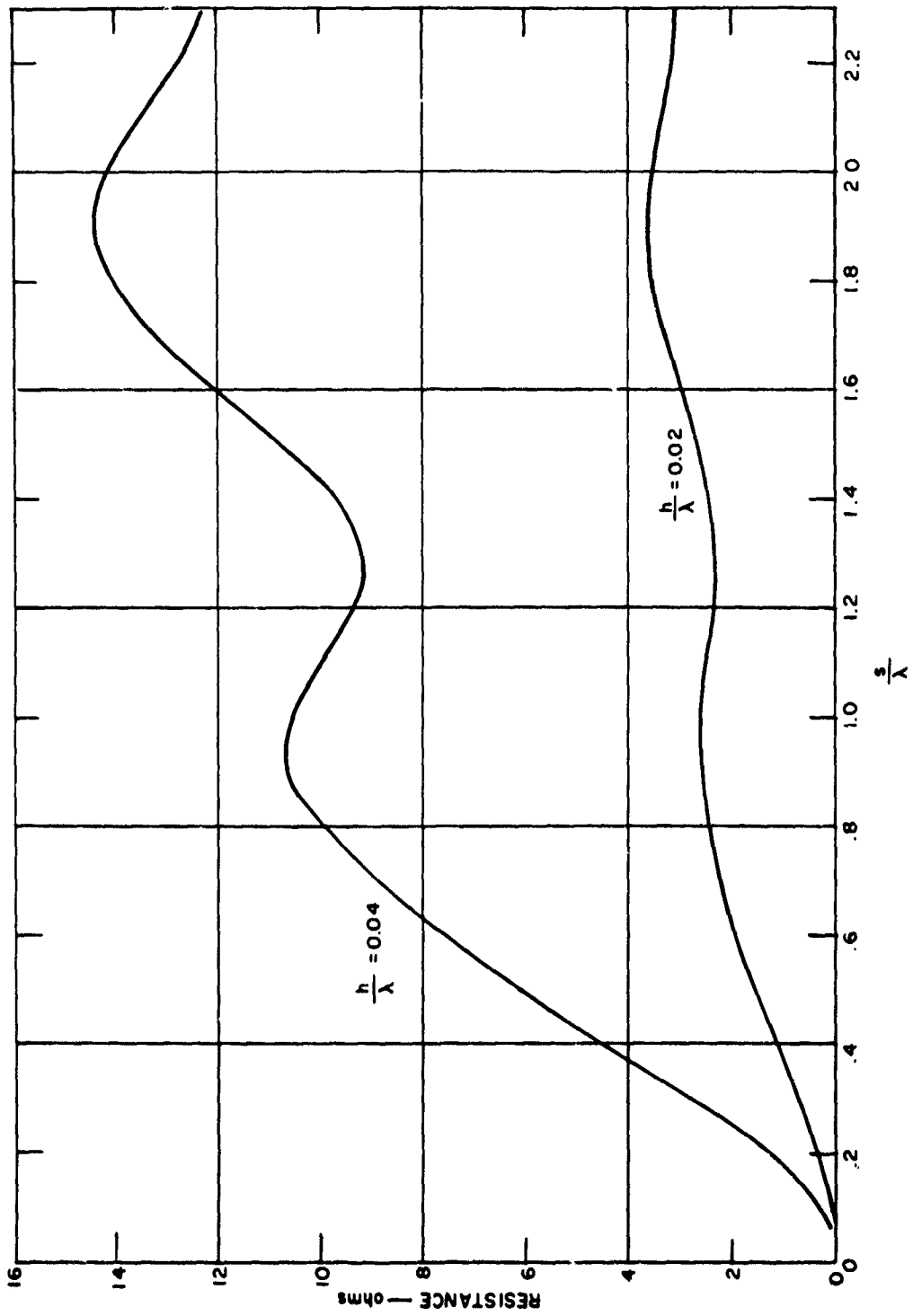


FIG. 35 RADIATION RESISTANCE OF A RECTANGULAR HALF-LOOP OVER A GROUND PLANE

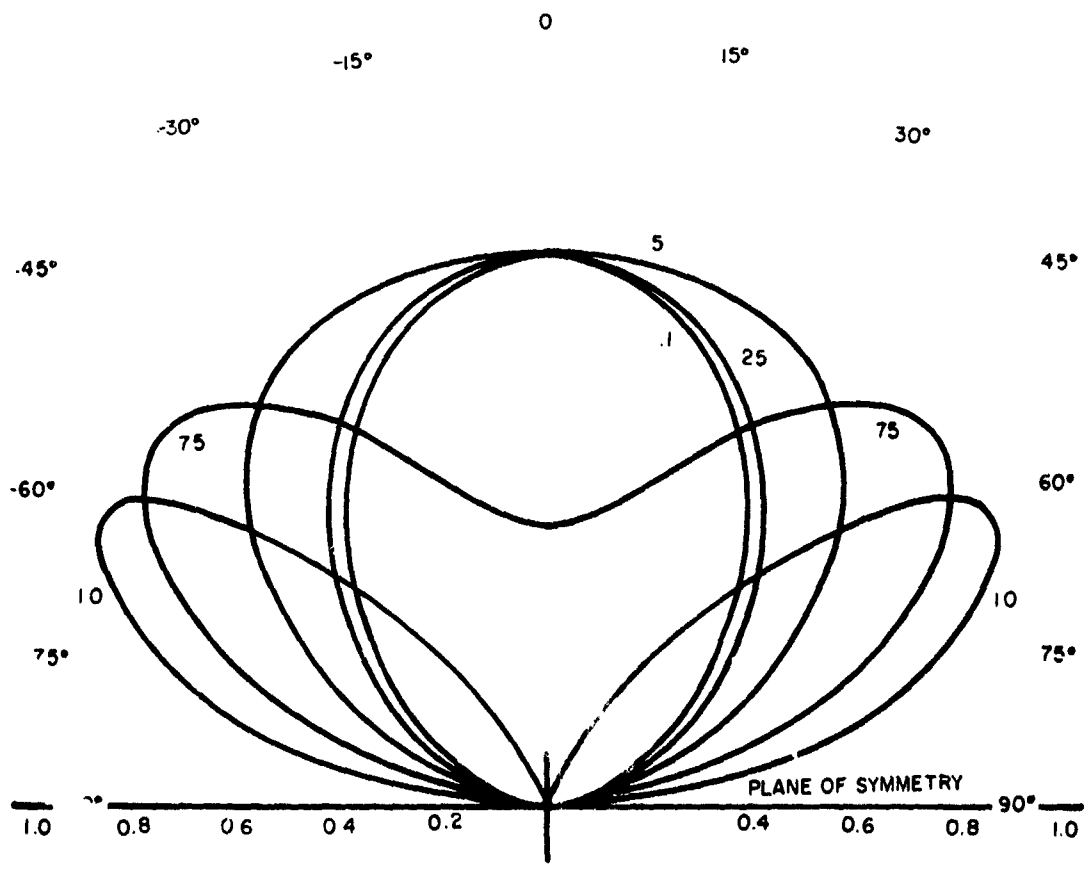


FIG. 36 H-PLANE RADIATION PATTERNS, VERTICAL POLARIZATION, FOR A RECTANGULAR LOOP OVER A GROUND PLANE, FOR VARIOUS DISTANCES OF SEPARATION OF THE VERTICAL SIDES, MEASURED IN WAVELENGTHS. Height above ground is 10^{-2} wavelengths in all cases.

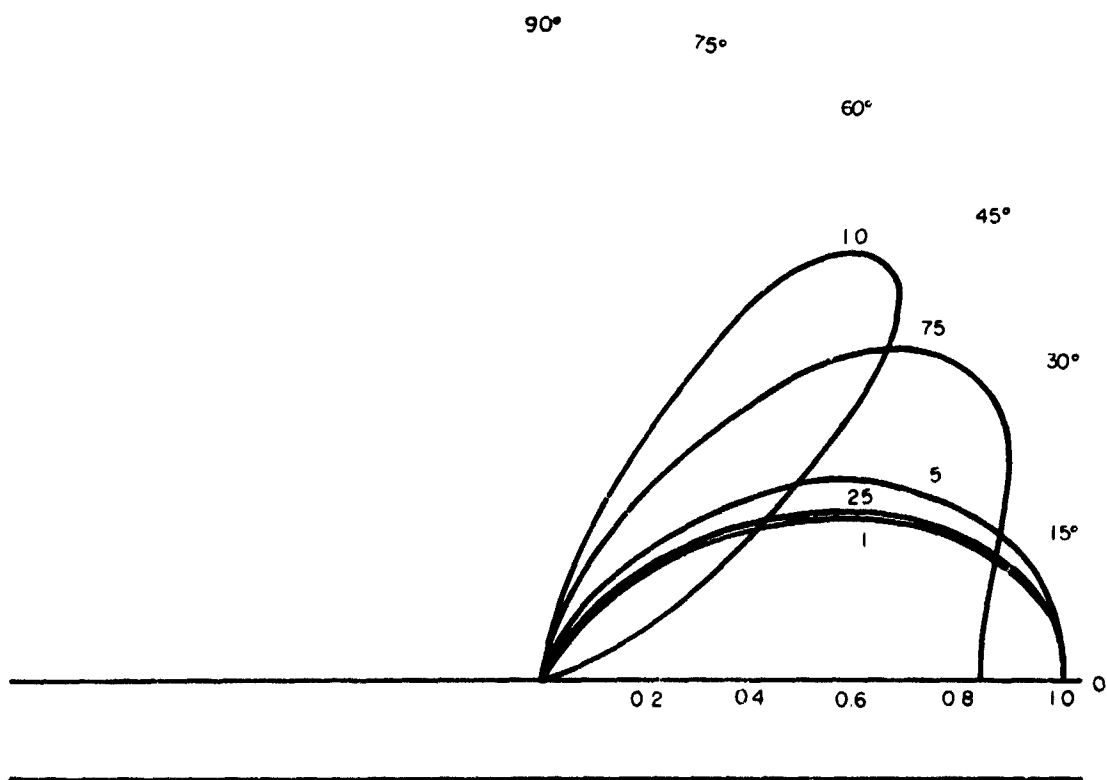


FIG. 37 E-PLANE RADIATION PATTERN, VERTICAL POLARIZATION, FOR A VERTICAL LOOP OVER A GROUND PLANE, FOR VARIOUS DISTANCES OF SEPARATION OF THE VERTICAL SIDES, MEASURED IN WAVELENGTHS. Height above ground is 10^{-2} wavelengths in all cases.

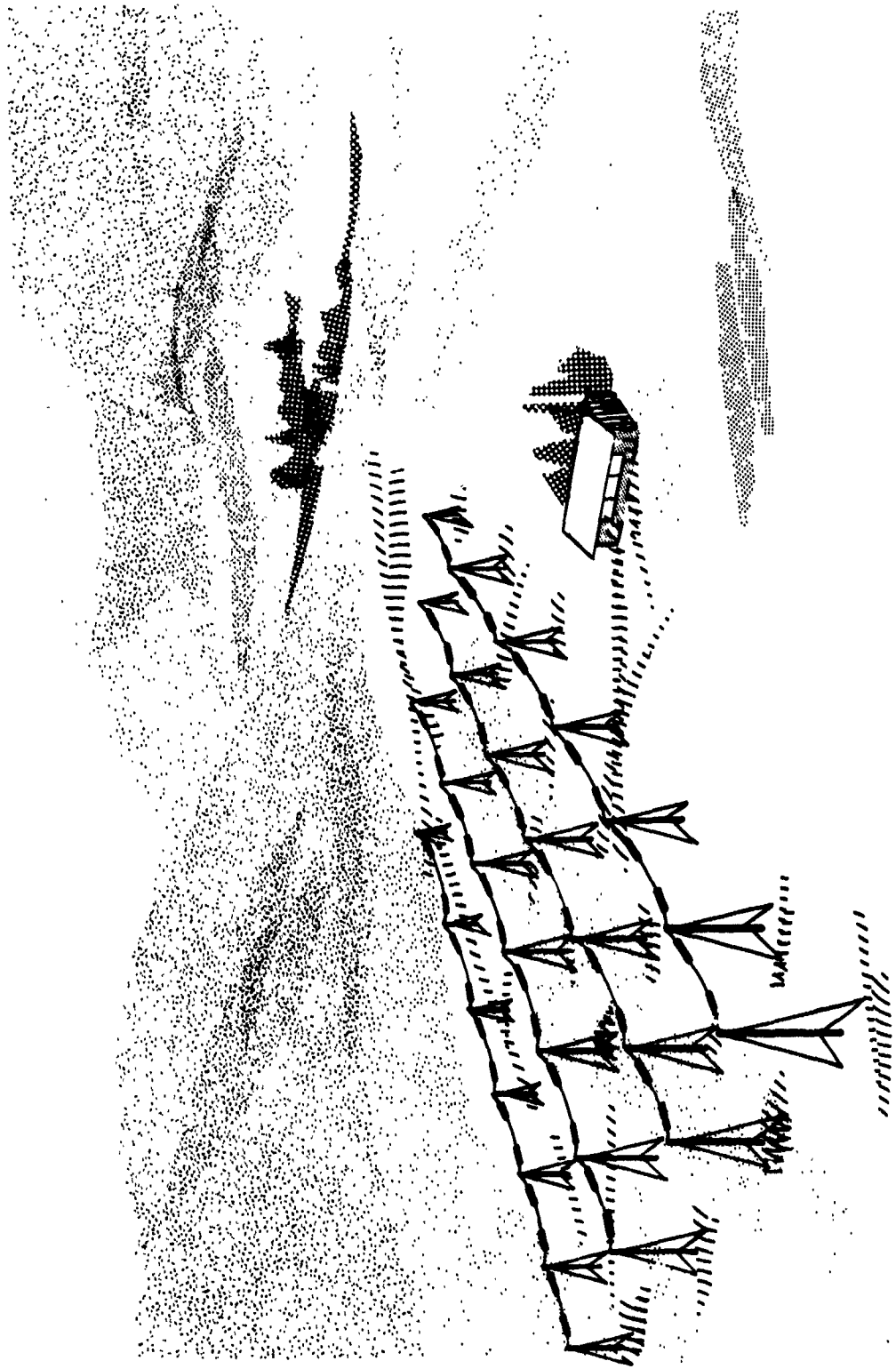


FIG. 38 SKETCH OF THE POSSIBLE APPEARANCE OF A MEGAWATT CW, HF TRANSMITTER

VI ACKNOWLEDGEMENTS

This research has been sponsored by the Advanced Research Projects Agency under ARPA Order 463, through the Office of Naval Research, Contract Nonr-4178(00).

REFERENCES

1. K. Landecker, and K. S. Imrie, "A Novel Type of High Power Pulse Transmitter," Aust. J. Phys. 13, pp. 638-654 (1960).
2. C. S. Franklin, U.S. Patent No. 1,304,868.
3. H. Raether, "Über eine gasionisierende Strahlung einer Funkenentladung" Z. Physik 110, pp. 611-624 (1938).
4. G. Schrank and G. Henry, "Spark-gap trigger system," Rev. Sci. Inst. 35, No. 10, pp. 1326-1331 (1964). Also, see F. Früngel, High speed pulse technology, p. 126 (Academic Press, New York, N.Y., 1965).
5. For example, J. M. Meek, and J. D. Craggs, Electrical breakdown of gases, Ch. 6 (Oxford Press, Oxford, England, 1953).
6. L. T. Dolphin, Jr., and A. F. Wickersham, Jr., "Very High Power VLF Systems," Tech. Memo. 1, Contract Nonr 4178(00), ARPA Order 463, SRI Project 4548, Stanford Research Institute, Menlo Park, California (January 1965).

UNCLASSIFIED

Security Classification

DOCUMENT CONTROL DATA - R&D		
<i>(Security classification of title, body of abstract and indexing annotation must be entered when the overall report is classified)</i>		
1. ORIGINATING ACTIVITY (Corporate author) Stanford Research Institute 333 Ravenswood Avenue Menlo Park, California		2a. REPORT SECURITY CLASSIFICATION UNCLASSIFIED
		2b. GROUP n/a
3. REPORT TITLE THE GENERATION OF MEGAWATT PEAK POWERS BY MODERN SPARK-TRANSMITTER TECHNIQUES		
4. DESCRIPTIVE NOTES (Type of report and inclusive dates) Final Report, February 1966		
5. AUTHOR(S) (Last name, first name, initial) Dolphin, Lambert T., Jr.; Wickersham, Arthur F., Jr.		
6. REPORT DATE February 1966	7a. TOTAL NO. OF PAGES 70	7b. NO. OF REFS 6
8a. CONTRACT OR GRANT NO. Nonr-4178(00)	9a. ORIGINATOR'S REPORT NUMBER(S) SRI Project 4548	
b. PROJECT NO. ARPA ORDER NO. 463	9b. OTHER REPORT NO(S) (Any other numbers that may be assigned this report)	
c.		
d.		
10. AVAILABILITY/LIMITATION NOTICES		
11. SUPPLEMENTARY NOTES		
12. SPONSORING MILITARY ACTIVITY Advanced Research Projects Agency		
13. ABSTRACT The demand for greater peak power for pulse radars has prompted the application of modern technology to the spark-gap transmitters of many years ago; in addition, working models have been built and tested of a spark transmitter recently invented in Australia. Working models have been tested at 6, 12, 23, 90, and 100 MHz with peak powers of 1/2 to 5 MW. The initial phase of a spark transmitter has been controlled to within 3 to 5 ns, permitting pulse-to-pulse coherence for Doppler radar. A pulse radar has been built using a 6 MHz spark transmitter; the output power, spectrum, and efficiency have been determined, and multiple ionospheric echoes have been observed. Bandwidth is about what would be expected for a pulse typically 1 μs long at 20 MHz. The spectrum is reasonably free of noise and harmonics; efficiencies lie between 10 and 25 percent. We conclude that peak powers as large as several gigawatts are possible. High-power operation may be achieved at frequencies as high as 100 to 200 MHz, and initial phase can be controlled to within a few tenths of a nanosecond. A 1 to 5 MW radar system using spark transmitters at 6, 12, and 23 MHz is now under construction.		

UNCLASSIFIED

Security Classification

14. KEY WORDS	LINK A		LINK B		LINK C	
	ROLE	WT	ROLE	WT	ROLE	WT
Spark transmitter Spark gap Spark ring Radar High power UHF Pressurized spark gap Ultraviolet trigger Pulse radar						

INSTRUCTIONS

1. **ORIGINATING ACTIVITY:** Enter the name and address of the contractor, subcontractor, grantee, Department of Defense activity or other organization (*corporate author*) issuing the report.
- 2a. **REPORT SECURITY CLASSIFICATION:** Enter the overall security classification of the report. Indicate whether "Restricted Data" is included. Marking is to be in accordance with appropriate security regulations.
- 2b. **GROUP:** Automatic downgrading is specified in DoD Directive 5200.10 and Armed Forces Industrial Manual. Enter the group number. Also, when applicable, show that optional markings have been used for Group 3 and Group 4 as authorized.
3. **REPORT TITLE:** Enter the complete report title in all capital letters. Titles in all cases should be unclassified. If a meaningful title cannot be selected without classification, show title classification in all capitals in parenthesis immediately following the title.
4. **DESCRIPTIVE NOTES:** If appropriate, enter the type of report, e.g., interim, progress, summary, annual, or final. Give the inclusive dates when a specific reporting period is covered.
5. **AUTHOR(S):** Enter the name(s) of author(s) as shown on or in the report. Enter last name, first name, middle initial. If military, show rank and branch of service. The name of the principal author is an absolute minimum requirement.
6. **REPORT DATE:** Enter the date of the report as day, month, year, or month, year. If more than one date appears on the report, use date of publication.
- 7a. **TOTAL NUMBER OF PAGES:** The total page count should follow normal pagination procedures, i.e., enter the number of pages containing information.
- 7b. **NUMBER OF REFERENCES:** Enter the total number of references cited in the report.
- 8a. **CONTRACT OR GRANT NUMBER:** If appropriate, enter the applicable number of the contract or grant under which the report was written.
- 8b, 8c, & 8d. **PROJECT NUMBER:** Enter the appropriate military department identification, such as project number, subproject number, system numbers, task number, etc.
- 9a. **ORIGINATOR'S REPORT NUMBER(S):** Enter the official report number by which the document will be identified and controlled by the originating activity. This number must be unique to this report.
- 9b. **OTHER REPORT NUMBER(S):** If the report has been assigned any other report numbers (*either by the originator or by the sponsor*), also enter this number(s).
10. **AVAILABILITY/LIMITATION NOTICES:** Enter any limitations on further dissemination of the report, other than those

imposed by security classification, using standard statements such as:

- (1) "Qualified requesters may obtain copies of this report from DDC."
- (2) "Foreign announcement and dissemination of this report by DDC is not authorized."
- (3) "U. S. Government agencies may obtain copies of this report directly from DDC. Other qualified DDC users shall request through _____."
- (4) "U. S. military agencies may obtain copies of this report directly from DDC. Other qualified users shall request through _____."
- (5) "All distribution of this report is controlled. Qualified DDC users shall request through _____."

If the report has been furnished to the Office of Technical Services, Department of Commerce, for sale to the public, indicate this fact and enter the price, if known.

11. **SUPPLEMENTARY NOTES:** Use for additional explanatory notes.
12. **SPONSORING MILITARY ACTIVITY:** Enter the name of the departmental project office or laboratory sponsoring (*paying for*) the research and development. Include address.
13. **ABSTRACT:** Enter an abstract giving a brief and factual summary of the document indicative of the report, even though it may also appear elsewhere in the body of the technical report. If additional space is required, a continuation sheet shall be attached.
 It is highly desirable that the abstract of classified reports be unclassified. Each paragraph of the abstract shall end with an indication of the military security classification of the information in the paragraph, represented as (TS), (S), (C), or (U).
 There is no limitation on the length of the abstract. However, the suggested length is from 150 to 225 words.
14. **KEY WORDS:** Key words are technically meaningful terms or short phrases that characterize a report and may be used as index entries for cataloging the report. Key words must be selected so that no security classification is required. Identifiers, such as equipment model designation, trade name, military project code name, geographic location, may be used as key words but will be followed by an indication of technical context. The assignment of links, roles, and weights is optional.